Methyl-torsion-facilitated internal energy delocalization following electronic excitation in *m*-fluorotoluene: Can *meta* and *para* substitution be directly compared?

Cite as: AIP Advances **10**, 125206 (2020); https://doi.org/10.1063/5.0032146
Submitted: 06 October 2020 . Accepted: 10 November 2020 . Published Online: 01 December 2020

Alexander R. Davies, David J. Kemp, and Timothy G. Wright

Methyl-torsion-facilitated internal energy delocalization following electronic excitation in *m*-fluorotoluene: Can *meta* and *para* substitution be directly compared?

Cite as: AIP Advances 10, 125206 (2020); doi: 10.1063/5.0032146
Submitted: 6 October 2020 • Accepted: 10 November 2020 •
Published Online: 1 December 2020

Alexander R. Davies, David J. Kemp, and Timothy G. Wright[a)]

AFFILIATIONS

School of Chemistry, University of Nottingham, University Park, Nottingham NG7 2RD, United Kingdom

[a)]Author to whom correspondence should be addressed: Tim.Wright@nottingham.ac.uk

ABSTRACT

Coupling between vibrations, and between vibrations and torsions—a generalization of intramolecular vibrational redistribution (IVR)—provides routes to internal energy delocalization, which can stabilize molecules following photoexcitation. Following earlier work on *p*-fluorotoluene (*p*FT), this study focuses on *m*-fluorotoluene (*m*FT) as probed via the $S_1 \leftrightarrow S_0$ electronic transitions and the $D_0^+ \leftarrow S_1$ ionization, using two-dimensional laser-induced fluorescence and zero-electron-kinetic energy spectroscopy, respectively. Wavenumbers are reported for a number of vibrations in the S_0, S_1, and D_0^+ states and found to compare well to those calculated. In addition, features are seen in the *m*FT spectra, not commented on in previous studies, which can be assigned to transitions involving vibration–torsion ("vibtor") levels. Comparisons to the previous work on both *m*-difluorobenzene and *m*FT are also made, and some earlier assignments are revised. At lower wavenumbers, well-defined interactions between vibrational and vibtor levels are deduced—termed "restricted IVR," while at higher wavenumbers, such interactions evolve into more-complicated interactions, moving toward the "statistical IVR" regime. It is then concluded that a comparison between *m*FT and *p*FT is less straightforward than implied in earlier studies.

I. INTRODUCTION

Anharmonic coupling in molecules leads to delocalization, and so dispersal, of internal energy within a molecule—an important aspect to enhanced photostability.[1–4] Which of the vibrations in a molecule can couple, and to what extent, depends on a number of factors, but having the same symmetry and being close in energy are two key considerations,[1] along with the relative motions of the atoms in those vibrations. Such coupling leads to actual vibrational motions having mixed character, and this can be discerned through an analysis of the vibrational activity in electronic and photoelectron spectra, where vibrational eigenfunctions of one electronic state are projected onto those of another. To first order, vibrational fundamentals do not couple anharmonically, but sometimes activity in fundamentals other than that excited can be seen in experimental spectra. This can be caused by changes in geometry that lead to significant Franck–Condon factors (FCFs), or as a result of Duschinsky rotations.[5]

Methylation in biomolecules has been invoked as a key factor in photoinduced carcinogenicity,[6] and consequently, an understanding of the role of methyl groups in the modification of a molecule's photobehavior is of key importance. Parmenter and coworkers have published numerous studies on the effect of methylation on intramolecular vibrational redistribution (IVR), with the most pertinent study here being that of Timbers *et al.*[7] In that work, it was concluded that *m*-fluorotoluene (*m*FT) undergoes intramolecular vibrational redistribution (IVR) more than an order of magnitude faster than *p*-fluorotoluene (*p*FT) and, hence, that the location of substituents is important in internal energy delocalization.

Recently, we published resonance-enhanced multiphoton ionization (REMPI) and zero-electron-kinetic-energy

(ZEKE) studies of the low-wavenumber regions of *m*FT[8] and *m*-chlorotoluene (*m*ClT),[9] which mainly focused on torsions and some vibration–torsion (vibtor) levels. The *m*FT study complemented the two-dimensional laser-induced fluorescence (2D-LIF) study of Stewart *et al.*,[10] who examined the first 350 cm^{-1} of the $S_1 \leftarrow S_0$ transition and the first 550 cm^{-1} of the $S_1 \rightarrow S_0$ transition via a mixture of LIF, dispersed fluorescence (DF), and 2D-LIF. In these studies, the spectra were assigned in terms of transitions involving torsional, vibtor, and vibrational levels in the S_0 and S_1 states. Earlier, Ito and co-workers[11–14] reported laser-induced fluorescence (LIF), DF, REMPI, and ZEKE spectra of the low-wavenumber region of *m*FT. Very recently, we compared the activity of three Duschinsky-mixed vibrations for *m*FT and *m*ClT, using a combination of 2D-LIF and ZEKE spectroscopy, finding that the spectra were exquisitely sensitive to small changes in molecular mass and electronic structure.[15]

Previously, we have studied the *p*FT molecule using REMPI, ZEKE, and 2D-LIF spectroscopy, showing how IVR evolves through the restricted to statistical regimes. It was seen that this is not a smooth evolution and that the methyl group plays a key role in this. We were able to identify key interactions and energy delocalization routes.[16–23]

In the present work, we extend our studies to the $S_1 \leftarrow S_0$ spectrum of *m*FT in the range 0 cm^{-1}–1350 cm^{-1} above the origin, using 2D-LIF, REMPI, and ZEKE spectroscopy. This encompasses a number of fundamental, overtone, combination, and vibtor levels. As with *p*FT, it is found that there is again an evolution from interactions between small numbers of levels, termed restricted IVR, at low wavenumber to widespread interactions, approaching statistical IVR, at higher wavenumbers. We identify specific interactions and derive wavenumbers for a number of vibrations across the S_0, S_1, and D_0^+ electronic states.

Over several years, our group has been examining the spectroscopy of fluoro-substituted and methyl-substituted benzene molecules. In doing so, we have examined the vibrational labeling of these molecules, putting forward general schemes for the ring-based vibrations of monosubstituted benzene molecules[24] and for each of the three isomeric classes of disubstituted benzene molecules.[25–27] These schemes were developed since neither Wilson[28]/Varsányi[29] nor Mulliken[30]/Herzberg[31] notations are appropriate. Indeed, separate schemes were required for these four classes of substituted benzene molecules, since the forms of the vibrations differ substantially between them. This implies that the comparison of vibrational activity between classes of substituted benzene molecules poses difficulties; however, the schemes do allow for direct comparison within each isomeric class. These labeling schemes are based on monofluorobenzene and difluorobenzene molecules, with consistent labels across both symmetric and asymmetric substitutions in the latter cases. They have allowed vibrational activity to be compared across spectra of *p*-difluorobenzene (*p*DFB), *p*-chlorofluorobenzene (*p*ClFB), *p*FT, and *p*-xylene (*p*Xyl)—see Refs. 17 and 32—although these ideas flow through our recent work across these molecules.

In the present case, a comparison will be made between the previously published detailed laser fluorescence study of *m*-difluorobenzene (*m*DFB)[33] and *m*FT, for which we expect the vibrational activity to be similar if the same vibrational numbering scheme is used—as will be seen, this expectation is largely borne out. Of course, the spectrum of *m*FT will be complicated by the contributions from torsion and vibtor levels, as noted above.

II. EXPERIMENTAL

The REMPI/ZEKE[34] and 2D-LIF[18] apparatuses are the same as those employed recently. In both experiments for *m*FT, a free-jet expansion of *m*FT (Sigma-Aldrich, 99% purity) in 2 bar Ar was employed.

For the 2D-LIF spectra, the free-jet expansion was intersected at $X/D \sim 20$ by the frequency-doubled output of a single dye laser (Sirah Cobra-Stretch), operating with Coumarin 503 and pumped with the third harmonic of a Surelite III Nd:YAG laser. The fluorescence was collected, collimated, and focused onto the entrance slits of a 1.5 m Czerny–Turner spectrometer (Sciencetech 9150) operating in single-pass mode, dispersed by a 3600 groove/mm grating, allowing ~300 cm^{-1} windows of the dispersed fluorescence to be collected by a CCD camera (Andor iStar DH334T). At a fixed grating angle of the spectrometer, the excitation laser was scanned, and at each excitation wavenumber, the camera image was accumulated for 2000 laser shots. This allowed a plot to be produced of fluorescence intensity vs both the excitation laser wavenumber and the wavenumber of the emitted and dispersed fluorescence, termed a 2D-LIF spectrum.[35,36] Band positions for the 2D-LIF spectra are given for the estimated band center.

For the REMPI and ZEKE spectra of *m*FT, the focused, frequency-doubled outputs of two dye lasers (Sirah Cobra-Stretch) were overlapped spatially and temporally and passed through a vacuum chamber coaxially and counterpropagating, where they intersected the free-jet expansion. The excitation laser was operated with Coumarin 503 and pumped with the third harmonic (355 nm) of a Surelite III Nd:YAG laser, while the ionization laser was operated with Pyrromethene 597 and pumped with the second harmonic (532 nm) of a Surelite I Nd:YAG laser. The jet expansion passed between two biased electrical grids located in the extraction region of a time-of-flight mass spectrometer, which was employed in the REMPI experiments. These grids were also used in the ZEKE experiments by application of pulsed voltages, giving typical fields of ~10 V cm^{-1}, after a delay of up to 2 μs; this delay was minimized while avoiding the introduction of excess noise from the prompt electron signal. The resulting ZEKE bands had widths of ~5 cm^{-1}–7 cm^{-1}. Electron and ion signals were recorded on separate sets of microchannel plates. Band positions for REMPI and ZEKE bands are given for the maximum, and ZEKE spectra were generally obtained when exciting through the intermediate band maximum.

For the REMPI spectrum of *m*DFB, a free-jet expansion of *m*DFB (Sigma-Aldrich, 99% purity) in 5 bar Ar was employed.

III. RESULTS AND ASSIGNMENTS

A. Nomenclature and labeling

1. Vibrational and torsional labeling

We shall employ the D_i labels[27] for the *m*FT vibrations, as used in Refs. 8–10; this C_s point group labeling scheme is based on the vibrations of the *m*DFB molecule. As such, we shall transcribe the Wilson/Varsányi labels in Ref. 11 and the C_{2v} Mulliken labels used

in Ref. 33 for *m*DFB to the D_i labels for the purposes of comparison with the present work. These, and the available experimental vibrational wavenumbers for *m*DFB, are presented in Table I, alongside the calculated wavenumbers—the calculated and experimental S_0 values are generally taken from Ref. 27 (some of which were deduced from Refs. 33 and 37), while the experimental values for the S_1 state were obtained from Ref. 33, with the calculated values for this electronic state being obtained in the present work.

TABLE I. Calculated and experimental wavenumbers (cm^{-1}) for the vibrations of *m*-difluorobenzene.

	S_0		S_1	
D_i (C_{2v})[a]	Calculated[b]	Expt.[c]	Calculated[d]	Expt.[e]
		a_1		
D_1 (1)	3122	3095		
D_2 (2)	3116	3086		
D_3 (21)	3112	3086		
D_4 (3)	3090			
D_5 (4)	1597	1611	1529	(1519)
D_6 (22)	1592	1613	1480	
D_7 (23)	1475	1490	1375	
D_8 (5)	1439	1435	1378	(1346)
D_9 (24)	1304	1337	1435	
D_{10} (6)	1255	1277	1250	
D_{11} (25)	1252	1292[f]	1228	1267[f]
D_{12} (26)	1145	1157	1118	1145
D_{13} (27)	1102	1120	1094	(1206)
D_{14} (7)	1058	1068	995	998
D_{15} (8)	994	1012	958	966
D_{16} (28)	941	956	883	936
D_{17} (9)	726	739	698	701
D_{18} (10)	514	522	438	442
D_{19} (29)	502	513	440	444
D_{20} (30)	467	477	462	468
D_{21} (11)	320	329	315	317
		a_2		
D_{22} (15)	963	957	719	(581)
D_{23} (12)	871	876	724	672
D_{24} (16)	856	857	362	480
D_{25} (17)	767	771	502	(479)
D_{26} (18)	671	680	457	422
D_{27} (13)	597	603	406	369
D_{28} (19)	455	454	241	260
D_{29} (14)	239	252	196	176
D_{30} (20)	222	227	98	127

[a]The D_i labels are described in Ref. 27, where the vibration mode diagrams can also be found. The values in parentheses are the Mulliken C_{2v} numbers used in Ref. 33 with 1–11 being a_1, 12–14 being a_2, 15–20 being b_1, and 21–30 being b_2.
[b]B3LYP/aug-cc-pVTZ, scaled by 0.97.[27]
[c]Taken from Ref. 27, where the selection and assignments are discussed; some of the values originate from Ref. 33. For D_{10}, we have reverted to the original liquid-phase value,[37] since we deduce that the reassignment of D_{11} in Ref. 33 is likely incorrect.
[d]TD-B3LYP/aug-cc-pVTZ, scaled by 0.97. Present work.
[e]Taken from Ref. 33; values in parentheses are those about which the authors of that work were less certain.
[f]Reassigned in the present work.

Since we shall also be referring to the methyl torsional motion for *m*FT, for which use of the G_6 molecular symmetry group (MSG) is appropriate, we shall employ those symmetry labels throughout. The torsional levels will be labeled via their *m* quantum number,[8,10] and the correspondence between the C_s point group labels and the G_6 MSG labels is given in Table II. To calculate the overall symmetry of a vibtor level, it is necessary to use the corresponding G_6 label for the vibration and then find the direct product with the symmetry of the torsion (Table II), noting that a C_{3v} point group direct product table can be used, since the G_6 MSG and the C_{3v} point group are isomorphic. The torsional levels in *m*FT are labeled with the signed quantum number *m* ($m = 0, 1, 2, \ldots$). The $m = 0$ level is singly degenerate, while levels with $|m| \neq 3n$ ($n = 1, 2, \ldots$) are doubly degenerate, consisting of +/− pairs, and levels with $m = 3n$ form linear combinations of the +/− pairs that split in energy under the influence of the torsional potential; these are labeled $m = 3(+)$ and $m = 3(-)$.[8]

Under the free-jet expansion conditions employed here, almost all molecules are expected to be cooled to their zero-point vibrational level, and thus essentially, all $S_1 \leftarrow S_0$ excitations are expected to originate from this level. In contrast, owing to nuclear-spin and rotational symmetry, the *m*FT molecules can be in one of the $m = 0$ or $m = 1$ torsional levels, with approximately equal population in each;[38] residual population in the $m = 2$ level is also seen.[8–10]

The available experimental vibrational wavenumbers for *m*FT are presented in Table III, alongside the calculated wavenumbers—the experimental S_0 values are generally taken from Ref. 27, while the experimental values for the S_1 state were obtained from Refs. 8 and 10 and the present work; the calculated S_0 and S_1 values are obtained in the present work and generally agree well with those presented in Ref. 10. The experimental values for the D_0^+ state are from Ref. 8 and the present work, while the calculated values are from the present work.

The level of theory employed is given in the footnotes of Tables I and III, and Gaussian 16[39] was used for all of these calculations.

2. Coupling and transitions

In the usual way, vibrational transitions will be indicated by the number, *i*, of the D_i vibration, followed by a superscript/subscript specifying the number of quanta in the upper/lower states, respectively. When required, torsional transitions will be indicated by *m*

TABLE II. Correspondence of the C_s point group symmetry classes with those of the G_6 molecular symmetry group. Also indicated are the symmetries of the D_i vibrations and the different pure torsional levels.[a]

C_s	G_6	D_i[b]	*m*
a'	a_1	D_1–D_{21}	0, 3(+), 6(+), 9(+)
a''	a_2	D_{22}–D_{30}	3(−), 6(−), 9(−)
	e		1, 2, 4, 5, 7, 8

[a]Symmetries of vibtor levels can be obtained by combining the vibrational symmetry (in G_6) with those of the pure torsional level, using the C_{3v} point group direct product table.
[b]The D_i labels are described in Ref. 27, where the vibration mode diagrams can also be found.

TABLE III. Calculated and experimental wavenumbers (cm^{-1}) for the vibrations of *m*-fluorotoluene.

	S_0		S_1		D_0^+	
D_i[a]	Calculated[b]	Expt.[c]	Calculated[d]	Expt.[e]	Calculated[f]	Expt.[g]
			a_1			
D_1	3107	[3081]	3128		3119	
D_2	3088	[3060]	3114		3107	
D_3	3086		3123		3111	
D_4	3072		3084		3092	
D_5	1578	[1595]	1512		1541	1569
D_6	1603	[1623]	1494		1490	
D_7	1479	[1492]	1392		1444	
D_8	1420	[1460]	1363		1385	
D_9	1302	[1295] 1294	1411		1356	
D_{10}	1239	[1251] 1254	1243		1299	1290
D_{11}	1271	[1266] 1271	1252	1260	1258	1275
D_{12}	1148	[1160] 1132	1122	[h]	1143	
D_{13}	1126	[1143] 1115	1113	[h]	1101	
D_{14}	1071	[1079] 1081	1023		1074	
D_{15}	988	[1003] 1004	958	965	997	984
D_{16}	912	[924] 930	866	840	873	874
D_{17}	720	[728] 731	685	684	700	710
D_{18}	519	[527] 525	459	460	509	510
$D_{19(X)}$	505	[513] 512	448	457	410	415
$D_{20(Y)}$	435	[450] 445	410	420	442	456
D_{21}	285	[296] 294	281	285	290	298
			a_2			
D_{22}	967	[970]	760		988	
D_{23}	886	[886]	705		916	
D_{24}	859	[858]	501		855	
D_{25}	773	[778] 775	575		787	780
D_{26}	683	[683]	468		592	592
D_{27}	557	[556] 554	377	367	514	517
D_{28}	443	[442] 441	241	253	373	380
D_{29}	236	[243] 237	184	174	190	190
D_{30}	199	[212] 201	122	128	167	169

[a]Labels are discussed in Ref. 27, where mode diagrams are presented. For D_{19} and D_{20}, the motions are very mixed in the S_1 state, as discussed in Ref. 15, and are denoted D_X and D_Y, respectively.
[b]B3LYP/aug-cc-pVTZ, scaled by 0.97. Present work—essentially the same as the values published in Ref. 10, which employed the same quantum chemical method.
[c]The values in square brackets are IR/Raman values that have been discussed in Ref. 27. Updates to some of these values have been made in gas-phase studies: Ref. 15 and the present work, in some cases confirming a value reported in Ref. 10.
[d]TD-B3LYP/aug-cc-pVTZ, scaled by 0.97. Present work—these values are close to the TD-B3LYP/cc-pVTZ values presented in Ref. 10, but several of the values do seem to be sensitive to the addition of diffuse functions to the basis set.
[e]Gas-phase values taken from Refs. 8 and 15 and the present work, in some cases confirming a value reported in Ref. 10.
[f]UB3LYP/aug-cc-pVTZ, scaled by 0.97; $\langle S^2 \rangle = 0.76$. Present work.
[g]Values taken from Refs. 8 and 15 and the present work.
[h]Experimental values for these two vibrations were reported in Ref. 11 but have been concluded to have been misassigned,[10] and we concur with this conclusion.[43].

followed by its superscripted value, and vibtor transitions will be indicated by a combination of the vibrational and torsional transition labels. When designating transitions, we shall generally omit the initial level, since it will be evident from either the jet-cooled conditions or the specified intermediate level.

As has become common usage, we will generally refer to a level using the notation of a transition, with the level indicated by the specified quantum numbers, with superscripts indicating levels in the S_1 state and subscripts indicating levels in the S_0 state. Since we will also be referring to transitions and levels involving the

ground state cation, D_0^+, we shall indicate those as superscripts, but with a single, additional, preceding superscripted "+" sign. Relative wavenumbers of the levels will be given with respect to the relevant zero-point vibrational level with $m = 0$, in each electronic state.

For cases where the geometry and the torsional potential are both similar in the S_1 and D_0^+ states, the most intense transition is usually expected to be that for which no changes in the torsional and/or vibrational quantum numbers occur, designated as $\Delta m = 0$, $\Delta\nu = 0$, or $\Delta(\nu, m) = 0$ transitions, as appropriate. However, as will be seen (and as reported in Refs. 8, 9, 14, and 15), the $\Delta m = 0$ and $\Delta(\nu, m) = 0$ transitions are almost always not the most intense bands in the ZEKE spectra for *m*FT, indicative of a significant change in the torsional potential upon ionization. The intensities of low-wavenumber features in the $S_1 \leftrightarrow S_0$ transitions have been discussed in Ref. 10, and reference will be made to that work when appropriate.

If two levels are close in wavenumber and have the same overall symmetry, then (except between vibrational fundamentals, to first order) interactions can occur, with the simplest example being the anharmonic interaction between two vibrational levels—the classic Fermi resonance.[40] Such couplings are only expected to be significant for small changes in the vibrational quantum number, $\Delta\nu \approx 3$, and for levels that lie close in energy.[41] For molecules that contain a hindered internal rotor, such as *m*FT and *p*FT, and if vibration–torsion coupling occurs, then interactions can also involve torsional or "vibtor" levels. This is expected to be significant only for changes in the torsional quantum number, Δm, of ±3 or ±6 in descending order of likely strength.[42] The result of such interactions is the formation of eigenstates with mixed character. Often, the resulting eigenstates will be referred to by the dominant contribution, with the context implying if an admixture is present.

B. An overview of the REMPI spectrum

In Fig. 1, we show the $S_1 \leftarrow S_0$ REMPI spectrum of *m*FT over the range 0 cm^{-1}–1350 cm^{-1}. It may be seen to be rich in structure, some of which has been assigned previously.[8,10–15] We note the good agreement with the appearance of the LIF spectrum in Ref. 11, which covers a similar range. Wavenumbers of some of the S_1 vibrations are in dispute.[10] We highlight that the 0 cm^{-1}–350 cm^{-1} region has been discussed in depth in Refs. 8 and 10, and the 400 cm^{-1}–480 cm^{-1} region was the focus in Ref. 15. Also in Fig. 1, we present the corresponding REMPI spectrum of *m*DFB, which compares very well with the LIF spectrum presented in Ref. 33.

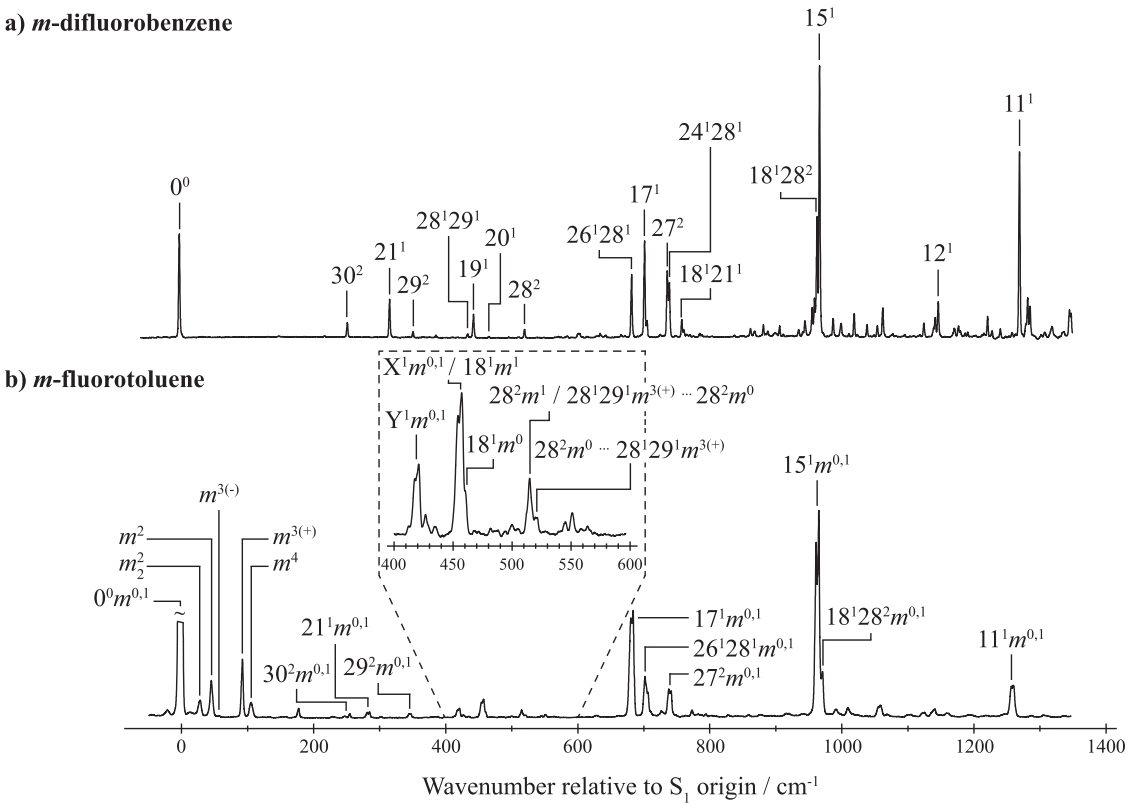

FIG. 1. Overview of the REMPI spectrum of the $S_1 \leftarrow S_0$ transition in the range 0 cm^{-1}–1350 cm^{-1} for (a) *m*DFB and (b) *m*FT. Only selected assignments are shown—see the text. For *m*FT, the origin bands, m^0 and m^1, have been truncated—see Ref. 8 for the 0 cm^{-1}–350 cm^{-1} region of the spectrum. The most intense bands in the expanded view were discussed and assigned in Ref. 15. See the text for further discussion on the assignments.

Overall, ignoring the torsional transitions for *m*FT, the correspondence between the main activity in both REMPI spectra in Fig. 1 is striking and adds confidence to the assignments for *m*FT discussed later.

A number of values and assignments in Table III are from the present work and will be discussed in Subsections III C–III G, where we break the discussion up into five main regions. Through these five regions, it will be seen that the coupling evolves from being absent, through well-defined coupling between a small number of levels at low wavenumber, into widespread coupling, approaching statistical IVR at higher wavenumbers.

In some of the figures, vertically integrated traces of the 2D-LIF spectra are presented. Each of these looks very similar to the corresponding section of the REMPI spectrum, confirming that the fluorescence collected is representative of the absorption spectrum in that region.

C. 2D-LIF and ZEKE spectra via the origin *m* = 0 and *m* = 1 levels

In Fig. 2, we show the 2D-LIF spectrum recorded when exciting through the pure torsional m^0 and m^1 excitations, and many assignments are also shown. The 0 cm^{-1}–550 cm^{-1} region of the emission spectrum has been assigned and discussed in depth by Stewart *et al.*,[10] and we concurred with those assignments in our ZEKE study.[8] In Ref. 10, only the 0 cm^{-1}–65 cm^{-1} region of the 2D-LIF spectrum via the m^0 and m^1 bands was presented, although DF spectra were presented up to 550 cm^{-1}, with full assignments. These will prove useful in assigning the 2D-LIF spectra in the present work, when we excite at higher wavenumbers.

The assignment of these vibrational bands allows S_0 vibrational wavenumbers to be established, which are included in Table III, some of which were reported by Stewart *et al.*[10] These values are close to those established by IR and Raman spectroscopy[37] and those discussed in Ref. 27, providing further confirmation of the assignments. Other features can be identified as vibtor levels associated with these vibrational transitions, and indeed, subject to sensitivity, we expect to see the main pattern of vibtor and related transitions that are observed for the origin, for each vibrational transition.

In Fig. 3, we show the ZEKE spectra recorded via both m^0 and m^1. The regions up to ~850 cm^{-1} were assigned in Ref. 8; in the present work, the spectra are extended up to ~1850 cm^{-1} and show more vibrational bands with their associated vibtor structure. As will be seen, these help in the assignment of other ZEKE spectra presented later. The vibrational wavenumbers arising from these spectra are also included in Table III.

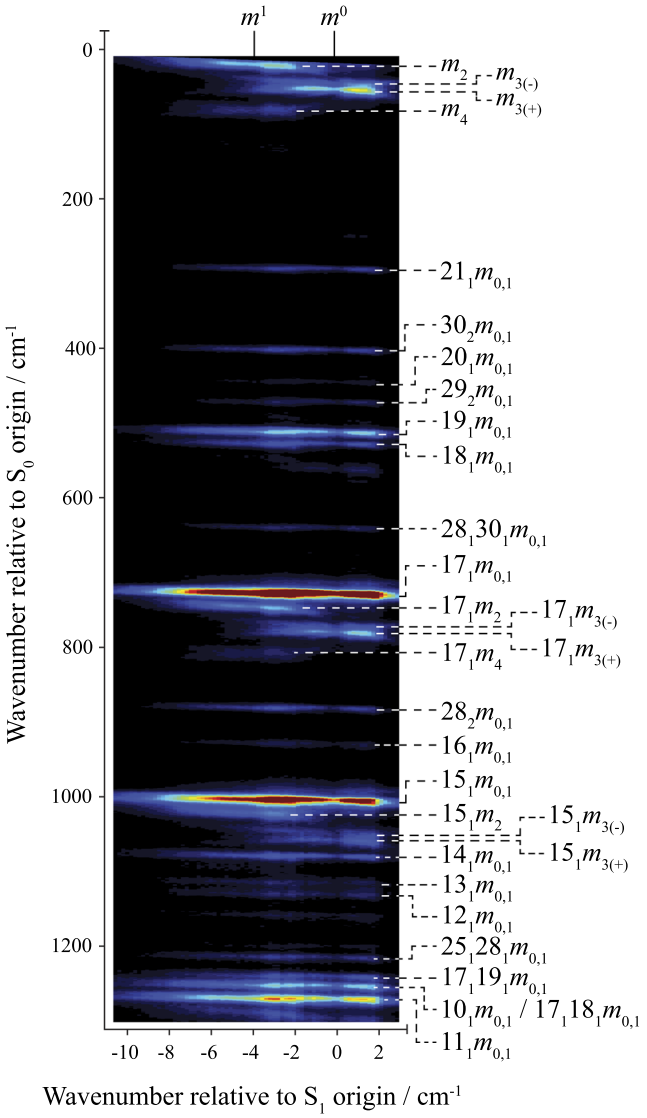

FIG. 2. 2D-LIF over the m^0 and m^1 excitation bands, showing the 0 cm^{-1}–1300 cm^{-1} emission region. Selected assignments are shown, with each main vibrational emission band being associated with a set of vibtor levels, many of which are indicated. See the text for further discussion on the assignments.

D. The 410 cm^{-1}–555 cm^{-1} region

The integrated 2D-LIF trace covering this region of the $S_1 \leftarrow S_0$ excitation is shown at the top of Fig. 4. The three most intense features in this region are Y^1 and the overlapped X^1 and 18^1 bands. The S_1 D_X and D_Y vibrations are highly mixed forms of the S_0 D_{19} and D_{20} vibrations, and these assignments, alongside the Duschinsky mixing that gives rise to the mixed character, have been discussed in Ref. 15. In Fig. 4, we also show an extended 2D-LIF spectrum recorded across this region. It can be seen that numerous features can be identified in the 2D-LIF image that are not obviously associated with discrete features in the integrated 2D-LIF (nor REMPI) spectrum; this highlights one aspect of the extra information that 2D-LIF spectra provide. The assignments of many of the bands are straightforward, combining the knowledge of the torsional levels from Refs. 8 and 10 and the vibrational levels from Ref. 15, and these are indicated in the figure, with numerous features arising from $\Delta(v, m) = 0$ transitions. However, there were also numerous cases where the assignment was less obvious, and some of these will be discussed in the following.

We see a 2D-LIF feature at (428, 675) cm^{-1}, whose assignment is to the $\Delta(v, m) = 0$ band ($28^129^1m^0$, $28_129_1m_0$). This assignment is reached on the basis of a weak associated band in the expected

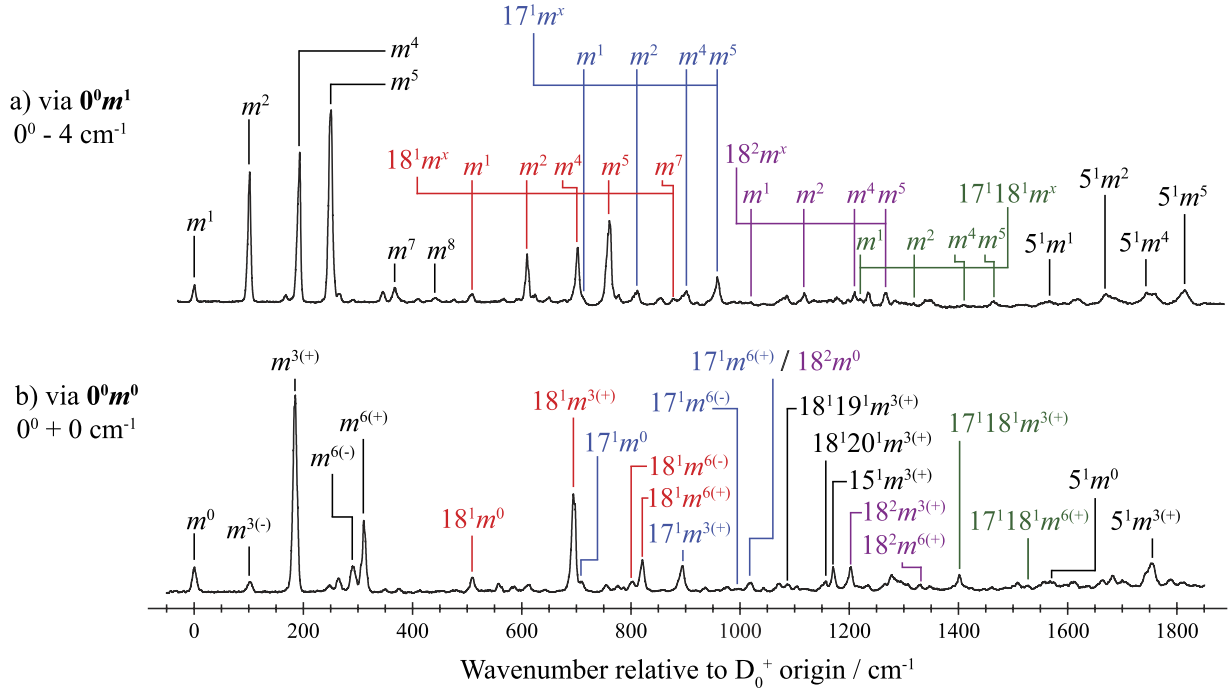

FIG. 3. ZEKE spectra via the (a) m^1 and (b) m^0 excitation bands. The preceding "+" sign used in the text is omitted from the assignments for clarity. These cover a wider range than those presented in Ref. 8, where further ZEKE spectra are shown when exciting though other torsional levels.

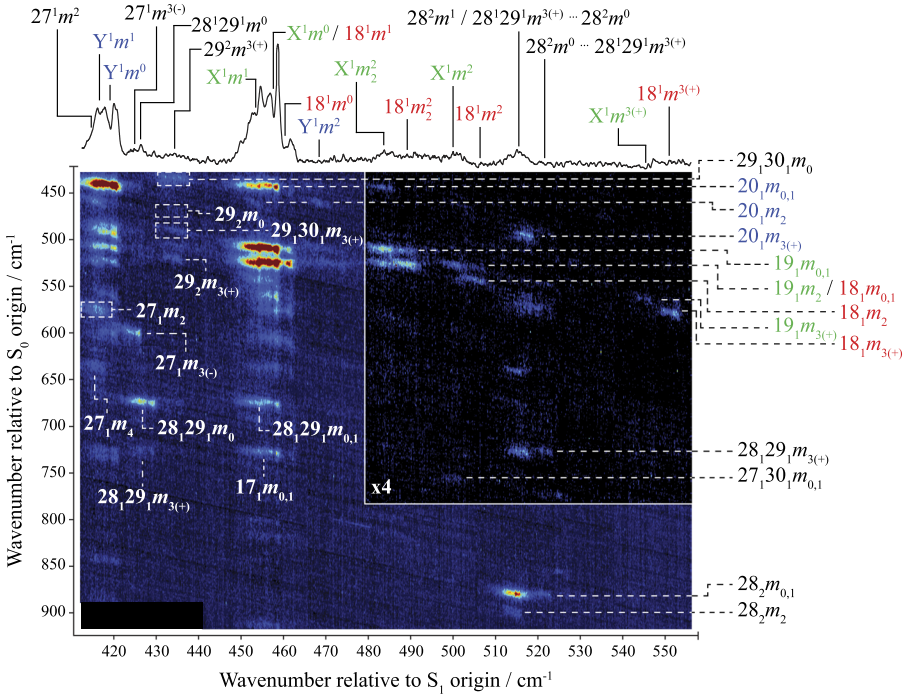

FIG. 4. 2D-LIF over the excitation range 410 cm^{-1}–555 cm^{-1}. At the top of the 2D-LIF spectrum, the trace shows the result of integrating vertically over the presented section of the 2D-LIF spectrum and closely resembles the corresponding region of the REMPI spectrum. The 415 cm^{-1}–465 cm^{-1} excitation range of the spectrum has been shown, and the main features are discussed and assigned, in Ref. 15. The majority of the vibtor structure and other 2D-LIF features whose assignments are indicated in white on the spectrum are presented here for the first time. The region between ~480 cm^{-1} and 550 cm^{-1}, as indicated, has been enhanced by 4× to highlight the weaker bands present in this region. Colored text is used for clarity. See the text for further discussion on the assignments.

position for $28_1 29_1 m_{3(+)}$ and also the ZEKE spectrum [Fig. 5(a)], which only shows the structure that is consistent with an $m = 0$ component. Furthermore, this is consistent with the observation of $28^1 29^1$ by Graham and Kable in the case of *m*DFB[33]—see Fig. 1(a).

Interestingly, there is no evidence for the corresponding $(28^1 29^1 m^1, 28_1 29_1 m_1)$ $\Delta(v, m) = 0$ band at this excitation position, and as just noted, the lack of the expected *e* symmetry bands in the ZEKE spectrum excludes the possibility of its being overlapped with the $m = 0$ component. It is interesting to note, however, that dual $m = 0$ and 1 component activity is observed for the corresponding emission when exciting at ~449 cm^{-1}–459 cm^{-1}. [This observation precludes an alternative assignment of the (428, 675) cm^{-1} band to a vibtor transition.]

Overall, this behavior is reminiscent of the fact that the $(29^1 30^1 m^1, 29_1 30_1 m_1)$ band was also observed to be very much weaker than $(29^1 30^1 m^0, 29_1 30_1 m_0)$.[10] The reason for the weakness of the transition involving $m = 1$ was not entirely clear, but the assigned $(29^1 30^1 m^1, 29_1 30_1 m_1)$ band was suggested as being significantly shifted from its expected excitation position,[10] and it was hypothesized that there could be a $29^1 30^1 m^1 \ldots m^7$ interaction, although this would be a $(\Delta v = 2, \Delta m = 6)$ interaction, and so perhaps this is not expected to be strong. In general terms, although we do expect more widespread vibtor coupling involving *e* symmetry torsions, there is no evidence of such coupling for the $28^1 29^1 m^1$ level in the 2D-LIF spectrum, and so the absence of the $m = 1$ component is somewhat puzzling.

In Fig. 5(a), we show the ZEKE spectrum recorded when exciting at 427 cm^{-1}, which shows a strong $\Delta m = 3$ band, $^+28^1 29^1 m^{3(+)}$, in line with expectations when exciting through totally symmetric vibrations;[8] there are also the expected weaker $^+28^1 29^1 m^0$ and $^+28^1 29^1 m^{6(+)}$ bands. There is no clear evidence for the ZEKE bands expected to arise from ionization from $28^1 29^1 m^1$, confirming that the major contribution to the REMPI spectrum at this wavenumber is indeed $28^1 29^1 m^0$.

We also see evidence in the 2D-LIF spectrum (Fig. 4) for bands associated with excitation of $27^1 m^2$ and $27^1 m^{3(-)}$. Evidence for the former arises from observation of $27_1 m_2$ and $27_1 m_4$ emission bands at excitation positions close to 415 cm^{-1}. We speculate that the $27^1 m^2$ level is interacting weakly with $Y^1 m^1$, which both have *e* symmetry; this is supported by their proximity in wavenumber, but also the extension of the emission bands underneath the $27^1 m^2$ excitation region. The $27^1 m^{3(-)}$ band is symmetry allowed [and is in line with $28^1 m^{3(-)}$ and $30^1 m^{3(-)}$ activity reported previously[8]], but this level could also be interacting with $Y^1 m^0$. The latter is supported by

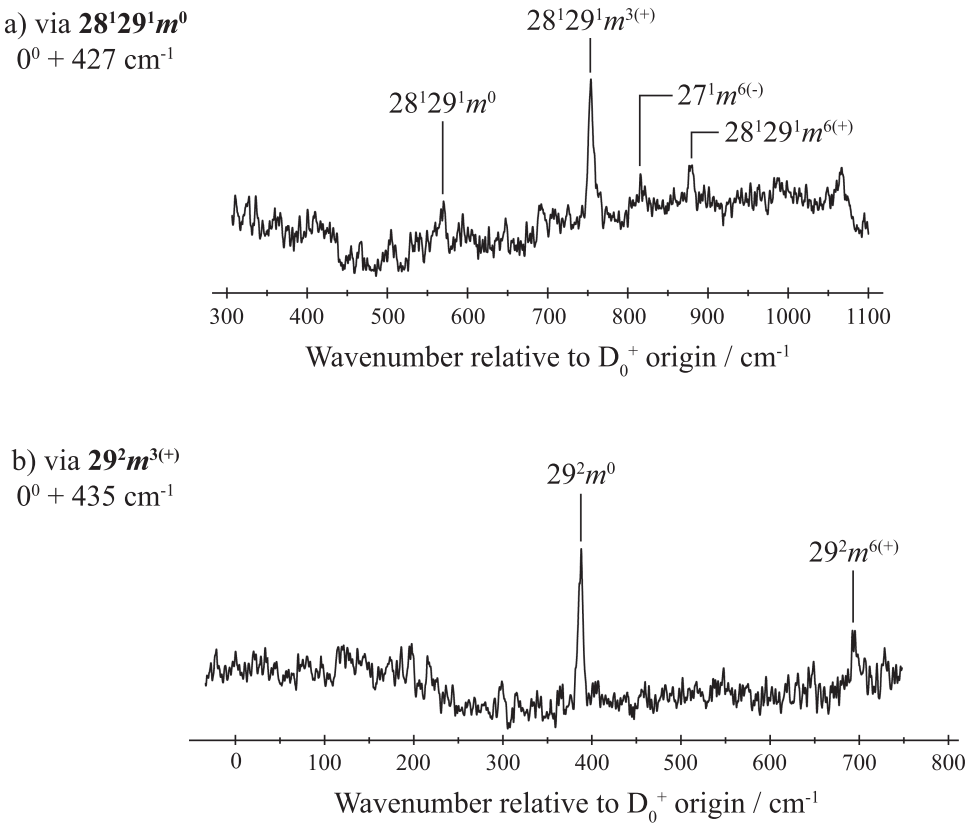

FIG. 5. ZEKE spectra recorded when exciting via the S_1 levels at (a) $0^0 + 427$ cm^{-1} and (b) $0^0 + 435$ cm^{-1}. The preceding "+" sign used in the text is omitted from the assignments for clarity. See the text.

there being $27_1 m_{3(-)}$ activity also at the $Y^1 m^0$ excitation position, and the "reverse" activity with the $20_1 m_0$ band extending to higher excitation wavenumbers. The width of the bands, and their limited activity, makes it difficult to ascertain whether shifts from expected band positions have occurred, which would be another signature of such an interaction.

Owing to the energetic closeness of the $27^1 m^{3(-)}$ and $28^1 29^1 m^0$ bands in the S_1 state (Fig. 4), it may be expected that when recording ZEKE spectra when exciting at $0^0 + 427$ cm^{-1}, we might also observe bands arising from excitation of $27^1 m^{3(-)}$. The weak feature at 816 cm^{-1} in the ZEKE spectrum when exciting here, shown in Fig. 5(a), is at about the expected wavenumber for the $\Delta m = 3$ band, $^+27^1 m^{6(-)}$, to which it is tentatively assigned. This is in line with the increased propensity of $\Delta m = 3$ transitions seen in the ZEKE spectra.[8] Overall, therefore, the ZEKE spectrum recorded when exciting at 427 cm^{-1} is consistent with the assignments shown in the 2D-LIF spectrum in Fig. 4 but is not definitive. In addition, even though the $27^1 m^{3(-)}$ and $28^1 29^1 m^0$ transitions overlap to some extent, no evidence of an interaction is seen.

A reasonable assignment for the weak 2D-LIF features in Fig. 4 that appear at an excitation wavenumber of 435 cm^{-1} can be proposed. This is close to the expected excitation wavenumber for $29^2 m^{3(+)}$, and a ZEKE spectrum recorded at this position, see Fig. 5(b), shows bands that are assignable to $^+29^2 m^0$ and $^+29^2 m^{6(+)}$. In line with observations in our previous paper,[8] the $^+29^2 m^{3(+)}$ band is expected to be weak and is not discernible in the spectrum.

The prominent feature at (514, 880) cm^{-1} in Fig. 4 is straightforwardly assignable as $(28^2 m^1, 28_2 m_1)$, based on the appearance of the corresponding $m = 2$ component at (515, 899) cm^{-1}. This is consistent with the observation of 28^2 in the case of *m*DFB.[33] Accompanying the prominent band is a weaker feature at (522, 879) cm^{-1}, which can be assigned as $(28^2 m^0, 28_2 m_0)$. It is initially surprising that this feature is so weak, as usually the $m = 0$ and $m = 1$ components for a vibrational band have comparable intensities, with the $m = 1$ band being slightly more intense (see Fig. 2). A clue as to the interpretation of these anomalous relative intensities comes from the ZEKE spectra, presented in Fig. 6, recorded at positions corresponding to the maxima of each of these features. The spectrum when exciting at 515 cm^{-1} is seen to be more complicated than the spectrum recorded at 520 cm^{-1}. With insight from the appearance of the ZEKE spectrum via m^1 [see Fig. 3(a)],[8] which demonstrates prominent $^+m^2$, $^+m^4$, and $^+m^5$ vibtor bands, and those via m^0 levels, which show prominent $^+m^{3(+)}$ and $^+m^{6(+)}$ vibtor bands [Fig. 3(b)], the bands arising from both the $28^2 m^1$ and $28^2 m^0$ levels can be straightforwardly identified. Two aspects of the spectra then become clear: first, there are bands arising from $28^2 m^0$ in both spectra, and second, there are other bands in the spectra. The $^+19^1 m^1$ and $^+20^1 m^1$ bands in the 515 cm^{-1} ZEKE spectrum, and the $^+21^1 29^1 m^{3(-)}$ band in the 520 cm^{-1} spectrum, arise from Franck–Condon (FC)-like activity; however, there are some other relatively intense bands that appear in both sets of spectra. Our favored assignment of these is to $^+28^1 29^1 m^x$ vibtor transitions, and their assignment suggests their source is $28^1 29^1 m^{3(+)}$, with the $^+28^1 29^1 m^{3(+)}/^+28^2 m^0$ band being clearly seen in Fig. 6(a), but not immediately in Fig. 6(b), where its position is indicated.

The expected position of $28^1 29^1 m^{3(+)}$ in S_1 is around 522 cm^{-1}, and this has the same symmetry, a_1, as the $28^2 m^0$ level, which is also expected to be close to this position; consequently, these two levels can interact. Furthermore, they differ by $\Delta v = 2$ and $\Delta m = 3$, making the suggested interaction sensible. We thus suggest a

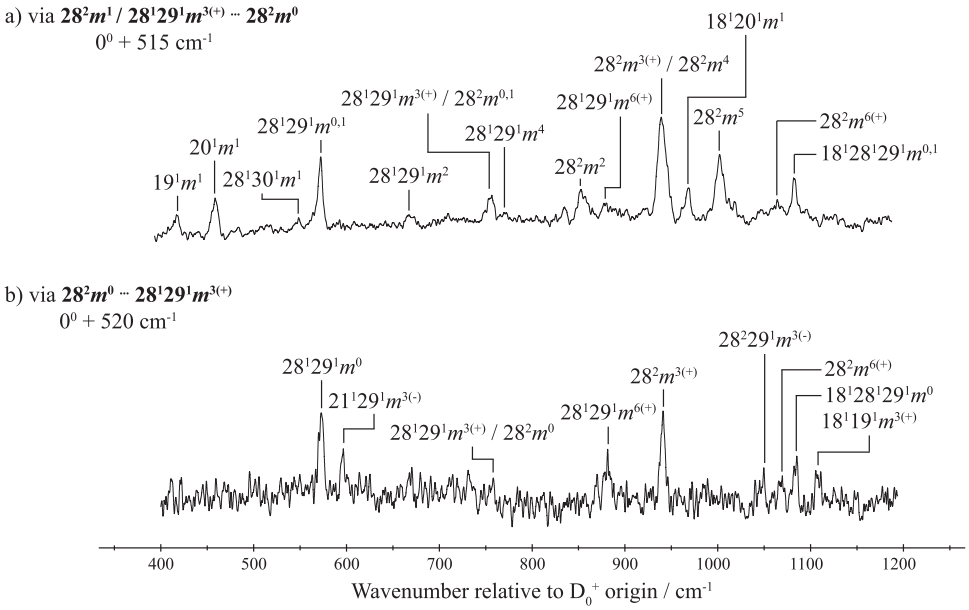

FIG. 6. ZEKE spectra of the $28^2 m^{0,1}$ bands: (a) $0^0 + 515$ cm^{-1} and (b) $0^0 + 520$ cm^{-1}. The preceding "+" sign used in the text is omitted from the assignments for clarity.

$28^2m^0\ldots28^129^1m^{3(+)}$ interaction that gives rise to two eigenstates of mixed composition. The relative intensities of the ZEKE bands suggest that the $28^2m^0\ldots28^129^1m^{3(+)}$ state (note that the leading term implies the dominant contribution to the eigenstate) gives rise to the higher, ~520 cm^{-1}, feature, while the $28^129^1m^{3(+)}\ldots28^2m^0$ eigenstate gives the lower feature; its transition is overlapped with that of 28^2m^1 at ~515 cm^{-1}, explaining the more-complicated structure in the ZEKE spectrum recorded at that position, Fig. 6(a).

This assignment is also consistent with the appearance of the 2D-LIF spectrum (Fig. 4), where the $28_129_1m_{3(+)}$ emission band has intensity across the 513 cm^{-1}–523 cm^{-1} region, consistent with the proposed interaction. We note the coincidence in the wavenumber of 17_1 and $28_129_1m_{3(+)}$, which makes the interpretation of the 2D-LIF spectrum less straightforward initially, but we accept the $28_129_1m_{3(+)}$ assignment based upon the ZEKE spectra and the $28_2m_{0,1}$ band profiles.

E. The 670 cm^{-1}–750 cm^{-1} region

The region of the REMPI spectrum of *m*FT between 670 cm^{-1} and 750 cm^{-1} can be seen to consist of three main features (Fig. 1), with the lowest wavenumber of these excitation bands being assigned to 17^1 (designated 1^1 by Okuyama *et al.*[11]). The other two features were assigned to 12^1 and 13^1 (designated $9b^1$ and $18b^1$ by Okuyama *et al.*[11]), but these two assignments have been questioned by Stewart *et al.*[10] When comparing to the *m*DFB spectrum (see Fig. 1), it can be seen that similar activity is seen, with Graham and Kable[33] having assigned these four main features to 26^128^1, 17^1, 27^2 and an overlapped feature consisting of 24^128^1 and 25^128^1. In a future paper,[43] we shall examine the two higher-wavenumber features in this region of the *m*FT spectrum in more detail, but for the purposes of the present work, we concentrate on the lowest wavenumber feature.

The integrated 2D-LIF trace is shown at the top of Fig. 7(c), which closely resembles the corresponding section of the REMPI spectrum. This excitation feature is assigned to the two *m* components of the 17^1 transition, in agreement with the assignment of Okuyama *et al.*[11] and consistent with the *m*DFB spectrum[33] (Fig. 1). Both the 2D-LIF spectrum [Fig. 7(c)] and the ZEKE spectra [Fig. 7(b)] support the 17^1m^1 and 17^1m^0 assignments; however, there are significant additional features in both spectra. Furthermore, although, when the 2D-LIF spectrum is examined, the strongest emission does indeed correspond to the two *m* components of 17_1, it is clear that the 17_1m_0 emission band is more intense

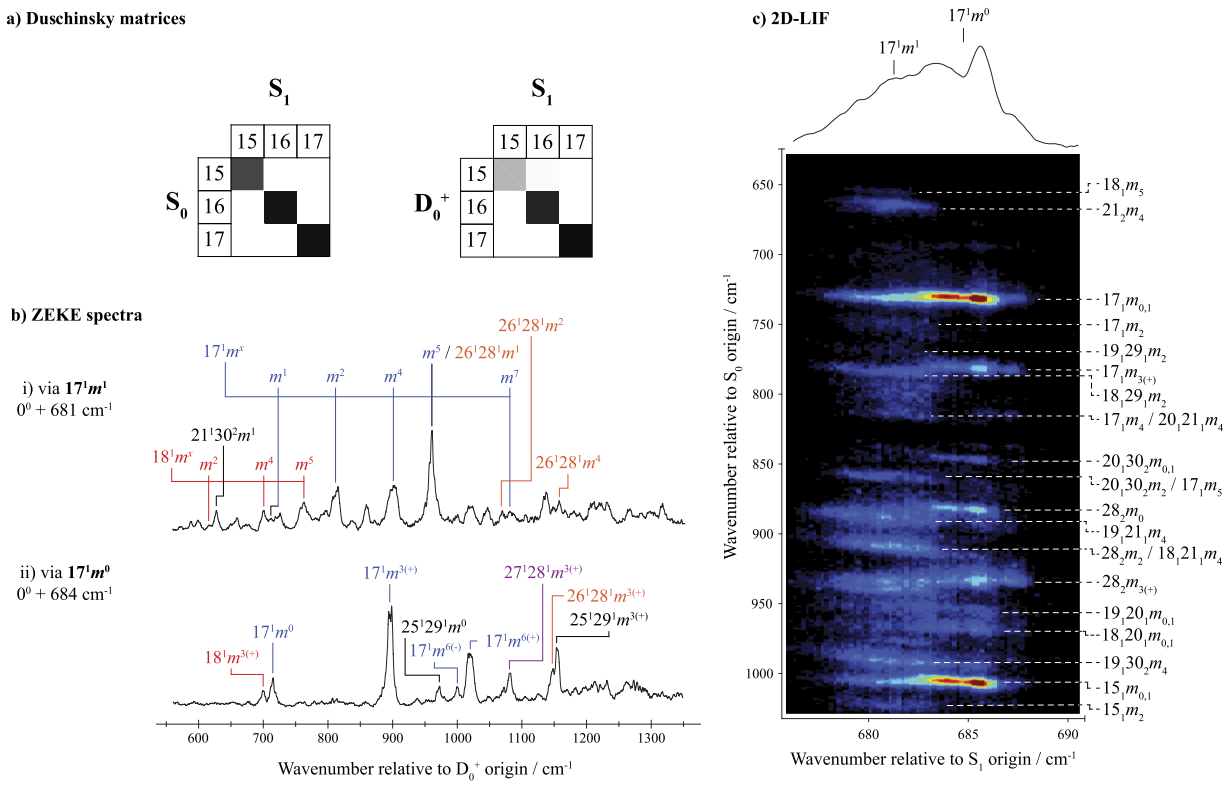

FIG. 7. (a) Duschinsky matrices showing the character of selected vibrations between excitation and ionization. The depth of shading represents the coefficients of mixing between vibrations in the two electronic states, between 0 (white) and 1 (black). (b) ZEKE spectra recorded at 0^0 + 681 and 0^0 + 684 cm^{-1}, which correspond to the m^1 and m^0 components of 17^1, respectively. The preceding "+" sign used in the text is omitted from the assignments for clarity. (c) 2D-LIF over the excitation range 673 cm^{-1}–690 cm^{-1}. At the top of the 2D-LIF spectrum, the trace shows the result of integrating vertically over the presented section of the 2D-LIF spectrum and closely resembles the corresponding region of the REMPI spectrum. Colored text is used for clarity. Selected assignments are shown, and the spectra are discussed further in the text.

than $17_1 m_1$—also reflected in the associated vibtor levels. The 15_1 bands are notably intense—cf. the 960 cm^{-1} feature (Sec. III F). Despite these observations, the Duschinsky matrices [Fig. 7(a)] indicate that there is almost no mixing between these modes during excitation or ionization. (In the matrices, the depth of shading of D_{15} implies that there is some predicted mode mixing of D_{15} between electronic states, but this is composed of several minor contributions from vibrational modes other than D_{17} and so is not discussed further here.) In contrast, via the origin, the m^1 band is more intense than m^0 (see Fig. 2), and this is the case with each vibrational emission band. We interpret this as an indication that the $17^1 m^1$ (e symmetry) S_1 level emits to more S_0 levels than $17^1 m^0$ (a_1 symmetry); furthermore, the ZEKE spectrum recorded via $17^1 m^1$ shows more bands than that recorded via $17^1 m^0$. Taken together, it is concluded that the $17^1 m^1$ level is likely interacting with other e symmetry levels.

In the 0 cm^{-1}–550 cm^{-1} emission region (not shown) of the 2D-LIF spectrum recorded via $17^1 m^{0,1}$, essentially all of the features seen via the origin (see Fig. 2 and Ref. 10) can also be seen. In the region shown in Fig. 7(c), emission to a number of vibrational levels and their associated vibtor levels can be seen, and a selection of assignments is shown.

The largely discrete nature of the emission spectrum suggests interactions will be between a small number of levels, and we initially considered an interaction with an $m = 2$ level for the most efficient coupling with $17^1 m^1$ ($\Delta m = 3$, recalling that the m quantum number is signed) and with $\Delta v \leq 3$. This led to the assignment of the emission band at (682, 784) cm^{-1} to $18_1 29_1 m_2$, which is supported by the observation of the weaker $19_1 29_1 m_2$ emission band at (682, 767) cm^{-1}. There are other emission bands that can be assigned when exciting at 682 cm^{-1}—these can be associated either with activity from $18^1 29^1 m^2$ or with further interactions between e symmetry levels in S_1. Although it is not possible to be definitive, the latter is supported by the fact that a number of levels are at a wavenumber position in S_1 that suggests that they could interact with $18^1 29^1 m^2$, each related by ≤ 3 changes in v and/or m. As such, we conclude that a number of concurrent stepwise interactions are occurring, which link $17^1 m^1$ to a number of e symmetry levels, explaining the significantly lower $17_1 m_1$ intensity compared to that of $17_1 m_0$. For example, $18^1 29^1 m^2$ can interact with $21^1 29^2 m^2$ via a $\Delta v = 3$ interaction, and the latter can then undergo a further $\Delta v = 3$ interaction with $29^3 30^1 m^2$. That multiple interactions are likely to be occurring is supported by the significant amount of underlying activity that can be seen in the 2D-LIF and ZEKE spectra in Fig. 7.

Another prominent band in the 2D-LIF spectrum is the band at (681, 665) cm^{-1}, which is assigned to $(21^2 m^4, 21_2 m_4)$, and we suggest $21^2 m^4$ is interacting with other e symmetry bands, including $17^1 m^1$, which would be $\Delta v = 3$, $\Delta m = 3$. At this excitation position, we also see other active bands, including $18_1 21_1 m_4$, $19_1 21_1 m_4$, and the overlapped $20_1 21_1 m_4$; at higher emission wavenumbers, we also see the $19_1 30_2 m_4$ band. We suggest that these bands arise from the $21^2 m^4$ activity.

In general, for solely anharmonic vibrational coupling, each m level of a particular vibration would behave similarly. However, in the case under discussion, the coupling is with a vibtor level that can only interact with one of the m levels of 17^1, and generally, there is a greater likelihood of coupling between e symmetry levels than for a_1 (or a_2)—see Sec. IV. Another possibility for an m-specific interaction with $17^1 m^1$ would be with the $m = 1$ level of an a_2 symmetry vibrational energy level, as the vibtor symmetry would then be e in both cases. However, the coupling mechanism could not simply be anharmonicity but would have to result from a breakdown in the separability of vibrational and torsional motions. It is also possible for m-specific interactions to occur with other vibtor levels of a_1 symmetry, but we do not see evidence of such interactions here.

The ZEKE spectrum via $17^1 m^1$, presented in Fig. 7(b)(i), is consistent, but not definitive, with regard to the suggested couplings: for example, although we do see $^+18^1 m^2$, we do not see a clear band for $^+18^1 29^1 m^2$, which would be expected at 805 cm^{-1} and, if present, would be overlapped by the $^+17^1 m^2$ band. Furthermore, the expected $\Delta m = 3$ ZEKE band would be $^+18^1 29^1 m^5$, anticipated at 952 cm^{-1}, which would overlap the $^+17^1 m^5$ band, and could contribute to the higher-than-expected intensity for this feature. In addition, bands associated with ionization from $21^2 m^4$ are all expected in positions that overlap with other bands. However, the greater complexity of the $m = 1$ ZEKE spectrum compared to that of $m = 0$ is consistent with m-specific coupling. Part of the difficulty in reaching definitive conclusions from the ZEKE spectra is that the significant change in the magnitude of the torsional barrier, coupled with the change in phase upon ionization, leads to activity arising from a number of m levels in the ZEKE spectrum for a specific m intermediate level.[8] For a limited amount of vibrational activity, this is actually a good assignment tool, as distinct patterns of bands can be identified for each FC active vibration. However, when interactions in S_1 have occurred, particularly those involving vibtor levels, the resulting increase in the number of bands leads to difficulties in reaching a definitive assignment. In both ZEKE spectra in Fig. 7(b), we have given suggested assignments to most of the intense bands at lower wavenumbers, and a number of these also appear in combination with $^+18^1$ at higher wavenumbers (not indicated). Also present in those spectra are bands that are assigned to combinations, and these appear to arise from FC-like activity.

F. The 952 cm^{-1}–976 cm^{-1} region

The relevant region of 2D-LIF and three ZEKE spectra recorded across this region are shown in Fig. 8. Okuyama *et al.*[11] assigned the main feature to 15^1 (denoted 12^1 in their work), and we concur with this assignment of the main excitation bands to $15^1 m^{0,1}$.

The integrated 2D-LIF spectrum is shown at the top of Fig. 8(b), which closely resembles this region of the REMPI spectrum. The 2D-LIF spectrum consists of a number of well-defined bands, falling into two main columns of activity, centered at excitation wavenumbers of 960 cm^{-1} and 964 cm^{-1}; a weaker column of activity is seen at excitation wavenumbers close to 970 cm^{-1}. Above about 1000 cm^{-1} in emission, there is a less well-defined structure extending across the spectrum, suggesting that this emission originates from coupled levels, which will be discussed below.

The band intensities in the 2D-LIF spectrum are not as expected, with the $17_1 m_x$ emission bands being significantly more intense than the $15_1 m_x$ emission bands; the assignment is clear, however, since the 17_1 bands were straightforwardly assigned above in Sec. III E, where we also commented that the 15_1 emission bands were unexpectedly intense when exciting 17^1. The assignment is also supported by the ZEKE spectra recorded at positions of the intermediate band maxima, 0^0 + 961 cm^{-1} and 0^0 + 965 cm^{-1} [Fig. 8(a)(i)

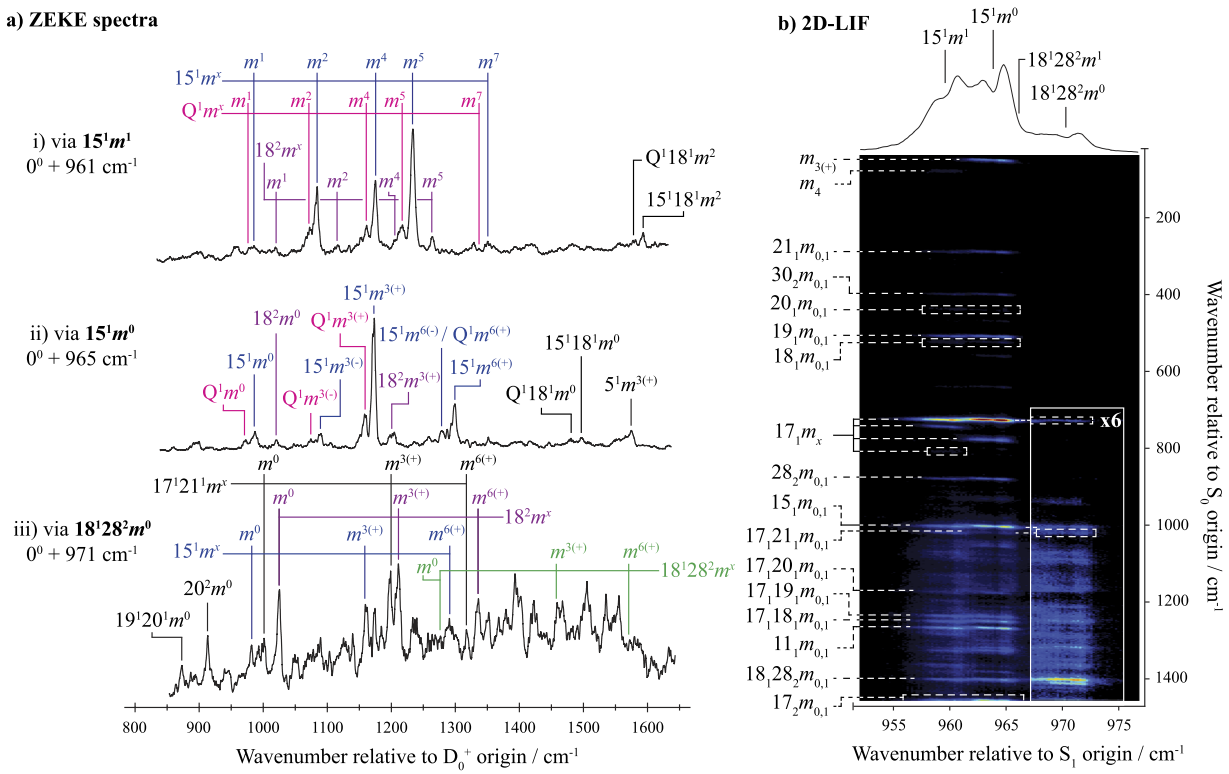

FIG. 8. (a) ZEKE spectra via 15^1m^1, 15^1m^0, and the feature at 0^0 + 971 cm^{-1}. In the ZEKE spectra, the preceding "+" sign used in the text is omitted from the assignments for clarity—see the text regarding the Q^1m^x bands. Colored text is used for clarity. (b) 2D-LIF over the excitation range 950 cm^{-1}–978 cm^{-1}. At the top of the 2D-LIF spectrum, the trace shows the result of integrating vertically over the presented section of the 2D-LIF spectrum and closely resembles the corresponding region of the REMPI spectrum. The region between 0^0 + 967 and 0^0 + 975 cm^{-1} has been enhanced by a factor of six, as indicated, as this structure is weak compared to the main activity. Selected assignments are shown—see the text for further discussion.

and Fig. 8(a)(ii)], which show the expected strong vibtor bands associated with $^+15^1$. We thus conclude that there are non-diagonal FCFs associated with emission from 15^1, which must be related to geometry changes, since we do not see evidence of a Duschinsky rotation between these vibrations in the Duschinsky rotation matrix [see Fig. 7(a)], and indeed, the ZEKE spectra [Fig. 8(a)] do not exhibit $^+17^1m^x$ bands; neither do we see $^+15^1m^x$ bands when exciting via $17^1m^{0,1}$ [see Fig. 7(b)]. The 2D-LIF spectrum [Fig. 8(b)] also shows significant torsional bands, together with vibtor bands associated with the main emissions. These are largely as expected, and their assignments are straightforwardly obtained both by the 2D-LIF spectrum obtained via m^0 and m^1 (Fig. 2) and by comparison with the work of Stewart *et al.*,[10] as well as the wavenumbers of other vibrations, obtained in the present work (see Table III).

When exciting at 970 cm^{-1}, the strongest 2D-LIF band is at (970, 1402) cm^{-1}. The assignment of this band to the $\Delta(v, m) = 0$ band ($18^128^2m^0$, $18_128_2m_0$) is relatively straightforward, fitting the expected wavenumbers in both the S_0 and S_1 states, and also being consistent with the 18^128^2 band seen for *m*DFB (Fig. 1). Furthermore, vibtor bands associated with $^+18^128^2m^0$ are seen in the ZEKE spectrum recorded when exciting via the intermediate band maximum 0^0 + 971 cm^{-1}, although it is noted that $^+18^128^2m^{3(+)}$ is not the most intense band in the spectrum, as would be expected. We note that the strongest emissions seen when exciting across 957 cm^{-1}–966 cm^{-1} all extend to higher excitation wavenumbers, consistent with either coincidental FC activity or an interaction between one or both $15^1m^{0,1}$ levels and a level at 970 cm^{-1}. Since the profile of the 18_128_2 emission band is strongest for the m_0 component, we suggest there is a $15^1\ldots18^128^2$ interaction for both *m* components, but for the $m = 1$ levels, further interactions cause a dissipation of the emission intensity across numerous transitions. In contrast, the interaction with $18^128^2m^0$ is weaker and less profligate, and so the emission band is more pronounced.

At this excitation wavenumber, we can also anticipate possible activity from other levels, including $17^121^1m^{0,1}$ and the vibtor levels $18^119^1m^{3(+)}$ and $18^120^1m^{3(+)}$. Relatively weak, but clearly observable bands at the correct wavenumbers for the $17_121_1m_{0,1}$ emissions can be seen in the 2D-LIF spectra; moreover, bands arising from $^+17^121^1m^x$ vibtor levels can also be seen in the ZEKE spectrum in Fig. 8(a)(iii). In addition, $^+18^2m^x$ ZEKE bands are seen, but these are thought to arise from FC activity, since these are also seen in other spectra when exciting fundamentals. In summary, it seems clear that interactions are occurring, and the evidence is that this predominantly involves the $m = 1$ components and involves widespread

coupling; the coupling with the m = 0 component is less definitive and is at best restricted in nature. The main activity comes from $15^1m^{0,1}$, but there is clear activity from $18^128^2m^{0,1}$ and persuasive evidence for involvement of $17^121^1m^{0,1}$; however, whether these levels are interacting significantly or not is less clear, but if they are, then the stronger interaction might be expected to be between 15^1 and 17^121^1, which is Δv = 3, while the other interaction would be Δv = 4.

The ZEKE spectrum recorded via 0^0 + 971 cm^{-1} [Fig. 8(a)(iii)] is rich in structure, and its assignment is challenging. We highlight that there are ZEKE bands at the correct position for $17^121^1m^0$ activity, for example, the intense $^+17^121^1m^{3(+)}$ band, but the corresponding activity expected for $17^121^1m^1$ is not seen, in line with comments in the previous paragraph. We note a strong series of bands at 1026 cm^{-1}, 1212 cm^{-1}, and 1338 cm^{-1} that appear to be the m = 0, 3(+), and 6(+) components associated with $^+18^2$, which are indicated in the figure. Although possible assignments could be put forward for other bands in this spectrum, we generally refrain from doing so, since these are not definitive. For example, in cases where an interaction can be suggested, such as $19^121^129^1m^{3(-)}$ and $18^121^129^1m^{3(-)}$, each being (Δv = 3, Δm = 3) from $17^121^1m^0$, it is not possible to identify all of the expected bands in this complicated spectrum.

Looking at the ZEKE spectra via 15^1m^x [Fig. 8(a)(i) and Fig. 8(a)(ii)], there are a series of bands labeled "Q^1m^x" and we show the Δv = 0 band as well as the corresponding vibtor structure. Despite these bands being well-resolved and prominent in both ZEKE spectra, there is no evidence for corresponding activity in the 2D-LIF spectrum. Although it is difficult to determine the identity of "Q," it may be associated with a level that is in Fermi resonance with $^+15^1$ in the cation (and so each corresponding pair of vibtor levels is also interacting); one promising candidate is Q = $^+25^129^1$. This could also simply arise from FC-like activity, of course, and we noted the appearance of $^+25^129^1m^x$ bands when exciting via 17^1m^1 [Fig. 7(b)].

In summary, at the very least, the 2D-LIF and ZEKE spectra suggest that there are likely numerous interactions occurring with the 15^1 level, supported by the appearance of many bands alongside those of $^+15^1m^x$ in the ZEKE spectrum recorded at 0^0 + 971 cm^{-1}. We also see clear evidence for $18^128^2m^0$ activity and persuasive evidence for $17^121^1m^0$.

G. The 1251 cm^{-1}–1266 cm^{-1} region

The 2D-LIF spectrum [Fig. 9(c)] consists of several well-defined bands on top of a broad background emission, particularly above

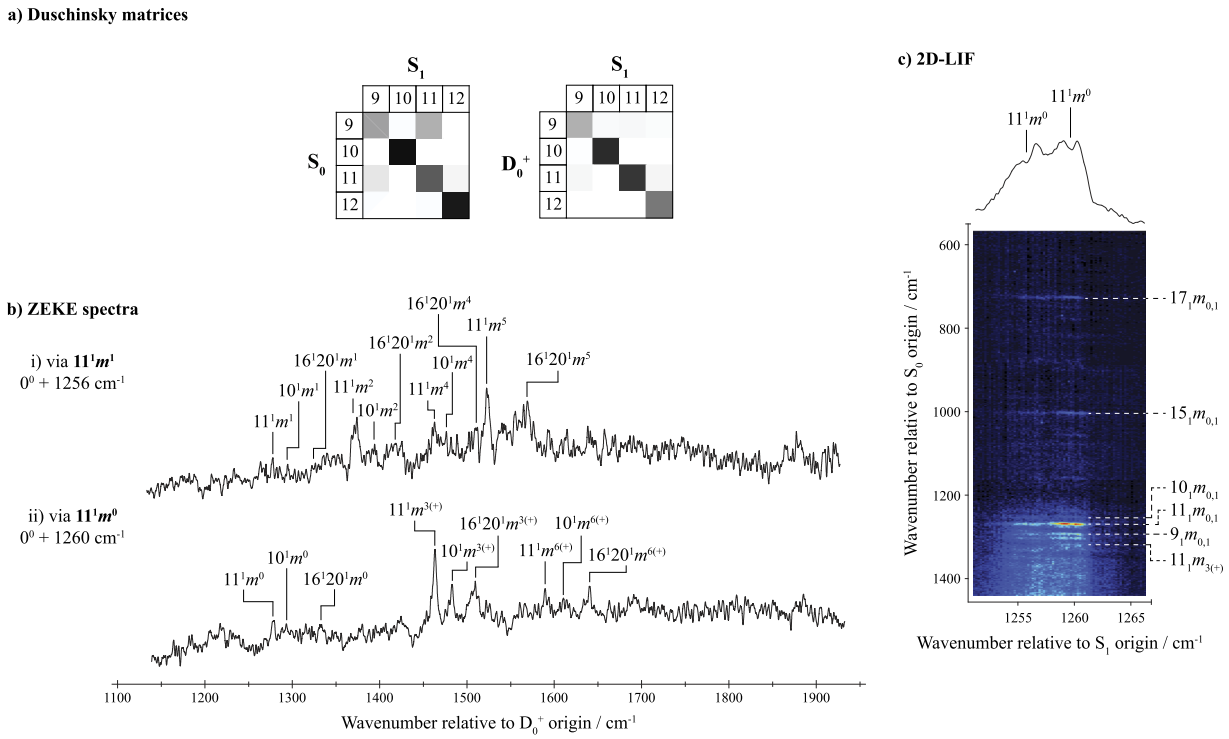

FIG. 9. (a) Duschinsky matrices showing the character of selected vibrations between excitation and ionization. The depth of shading represents the coefficients of mixing between vibrations in the two electronic states, between 0 (white) and 1 (black). (b) ZEKE spectra via 11^1m^1 and 11^1m^0. In the ZEKE spectra, the preceding "+" sign used in the text is omitted from the assignments for clarity. (c) 2D-LIF over the excitation range 1250 cm^{-1}–1267 cm^{-1}. At the top of the 2D-LIF spectrum, the trace shows the result of integrating vertically over the presented section of the 2D-LIF spectrum and closely resembles the corresponding region of the REMPI spectrum. Selected assignments are shown, and the spectra are discussed further in the text.

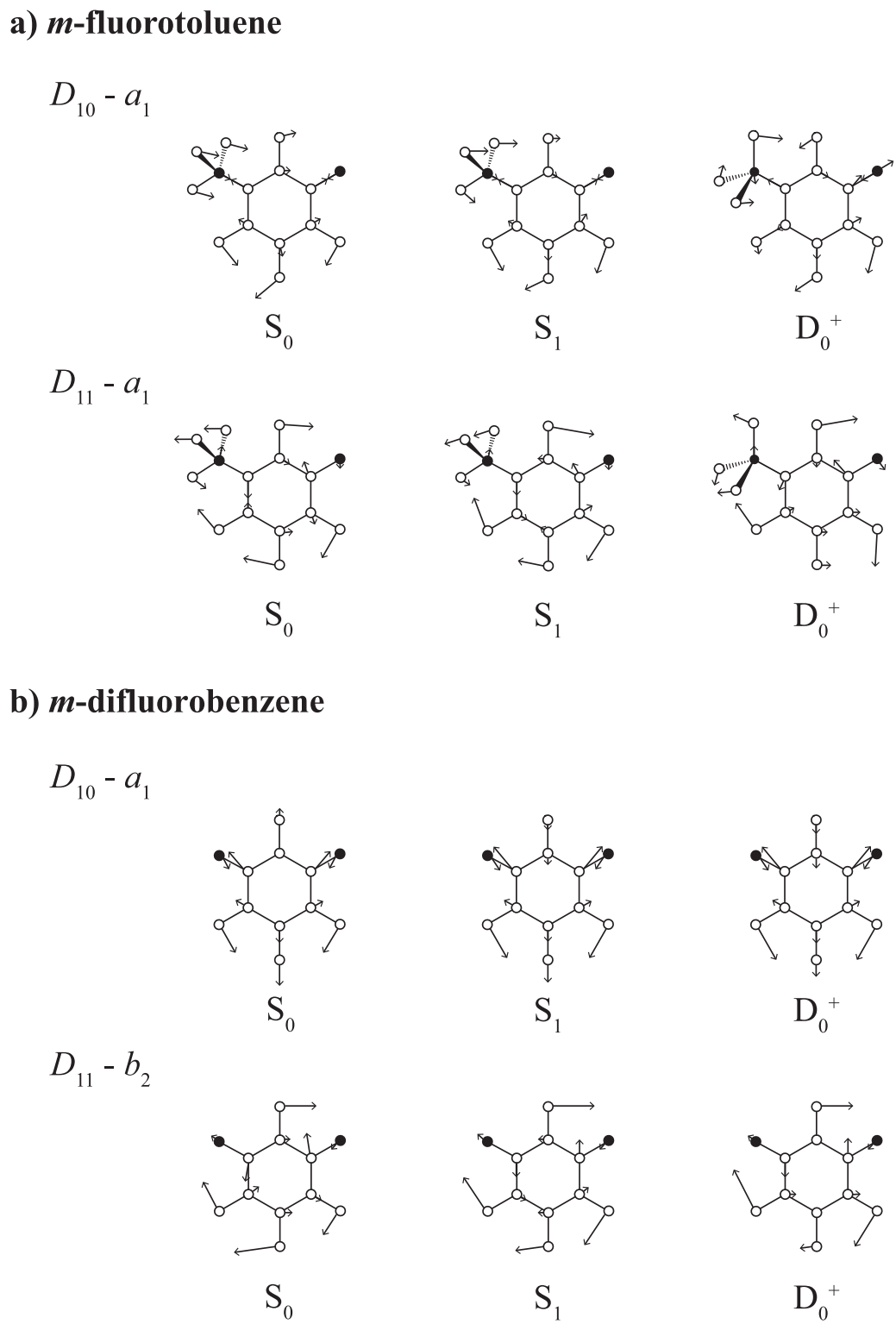

FIG. 10. Calculated mode diagrams for the D_{10} and D_{11} vibrations of (a) *m*FT (G_6) and (b) *m*DFB (C_{2v}) in the three electronic states under consideration, obtained using quantum chemistry calculations, as indicated in Tables I and III (for *m*DFB, the level of theory used for the cation was the same as that used for *m*FT). The motions are distinctive, and hence, assigning each vibration from the mode diagram is straightforward.

1200 cm^{-1}, and the integrated spectrum at the top of the spectrum closely resembles this region of the REMPI spectrum.

The main emission band for *m*FT, when exciting across 1254 cm^{-1}–1262 cm^{-1}, is at 1271 cm^{-1}. Comparing this value with the liquid-phase IR/Raman values suggests an assignment of the emission to 11_1, and this would be in line with the calculated wavenumbers. Note that Okuyama *et al.*[11] assigned a value of 1267 cm^{-1} to an S_0 vibration, which they labeled ν_{14} in Varsányi[29] notation and would correspond to *m*DFB mode ν_{25} in Mulliken notation[33] and, hence, D_{11} here; however, it was shown in previous work that Varsányi modes ν_3 and ν_{14} have got confused over the years and, further, that these labels do not describe the motions of the atoms in disubstituted benzene molecules.[24,25] With these caveats, the present assignment and that of Ref. 11 are in agreement. In Fig. 10, we show the calculated motions of D_{10} and D_{11} for *m*DFB and *m*FT in each of the three electronic states, showing that their motions are distinctive and, hence, assignment of each from the calculations is unambiguous.

A comparison of the REMPI spectrum of *m*FT with that of *m*DFB also suggests that the excitation at 1267 cm^{-1} should be assigned as 11^1; however, this was assigned as 10^1 (denoted 6^1) in the fluorescence study.[33] In *m*DFB, under C_{2v} point group symmetry, the D_{10} vibration is of a_1 symmetry, while that of D_{11} is b_2; thus, the 10^1 transition would be symmetry allowed. However, other transitions involving b_2 symmetry vibrations were assigned in Ref. 33, with 21^1, 19^1, and 20^1 transitions being notable; these are likely to be vibronically induced. These are also all seen in *m*FT[15] (where they all become symmetry allowed), but also the 18^1 transition is moderately intense in *m*FT but is absent in the *m*DFB spectrum (see Fig. 1 and Ref. 33), even though D_{18} is totally symmetric in both molecules. Hence, there is no prima facie reason not to assign the *m*DFB transition at 1267 cm^{-1} to 11^1, which would bring consistency with the *m*FT assignment. We highlight that Table I shows that the calculated values for D_{10} and D_{11} in the S_0 state of *m*DFB are too close to be discriminant (but their motions and so identities are clear—see Fig. 10), and with either assignment, there is a 40 cm^{-1} difference between the calculated value and the experimental value. Additionally, we are particularly cautious regarding the calculated S_1 values, which we have found to be often less reliable than those for the S_0 and D_0^+ states.[23,44]

Further evidence is gleaned from related symmetrically substituted molecules: in Ref. 27, vibrational wavenumbers are presented for five such molecules. Excluding *m*DFB, the wavenumber for the D_{10} vibration lies below that of D_{11} for both the experimental and calculated values for all of the other molecules. For *m*DFB, as noted, the calculated values are only a few cm^{-1} apart, but the experimental values, as assigned, are clearly reversed compared to those of the other molecules. Given the variation in these wavenumbers with mass—and given that the corresponding values for *m*-xylene and resorcinol are consistent with each other, but the reverse of the previously assigned values for *m*DFB—we suggest that the D_{10} and D_{11} assignments need to be reversed as well, and this has been done in Table I. This is then consistent with the *m*FT results obtained herein. Consequently, as with 18^1, it appears that 10^1 simply is not active in *m*DFB, despite being totally symmetric, while we conclude that 11^1 must be vibronically active. Furthermore, we note that Graham and Kable[33] have commented that previous assignments of the b_2 symmetry vibrations of *m*DFB are questionable, noting that the assignment of 11^1 in S_1 to a value of 1608 cm^{-1} does not seem to be correct, and indeed, this would not agree well with the calculated value in Table I.

In summary, the most intense 2D-LIF band for *m*FT in Fig. 9(c) at (1260, 1271) cm^{-1} is assigned as (11^1m^0, 11_1m_0) and is significantly more intense than the corresponding $m = 1$ band. The ZEKE spectra [Fig. 9(b)] are consistent with this assignment, with the main bands being assigned as the expected vibtor levels via the two *m* components. Several other fundamentals are also seen, and, where the sensitivity allows, the expected associated vibtor structure is seen.

With the assignment of the excitation to 11^1, the observed structure in the ZEKE spectrum allows a vibrational wavenumber of 1275 cm^{-1} to be obtained for $^+11^1$. (We note that, unhelpfully, the experimental value for this vibration falls between the calculated values for $^+11^1$ and $^+10^1$, and so this cannot be used as further evidence for this assignment, which is largely based on the 2D-LIF spectrum—see Table III.) The ZEKE spectra have a significant underlying unstructured signal, which is akin to the broad background in the 2D-LIF spectrum and again is consistent with significant IVR occurring. Another progression of vibtor levels is also seen in both ZEKE spectra, consistent with a vibration with the wavenumber 1330 cm^{-1}, which can be plausibly assigned to $^+16^120^1$, which could be arising from a $\Delta v = 3$ interaction; the activity in $^+10^1$ likely arises from FC activity, since the Duschinsky matrices, Fig. 9(a), show that D_{10} and D_{11} are not significantly mixed upon ionization. If the $^+16^120^1m^x$ assignments are correct and an interaction is indeed occurring, then this suggests a value for D_{16} in S_1 of ~840 cm^{-1}, which is in fair agreement with the calculated value. The interaction would be expected for both *m* components, which is consistent with the ZEKE spectrum. The 16_120_1 bands, expected at ~1370 cm^{-1}, are in a region of the 2D-LIF spectrum that consists of unstructured emission, effectively ruling out the possibility of definitive identification. This emission, together with the unstructured background in the ZEKE spectra, suggests significant interactions are occurring, but we cannot provide unambiguous assignments for all of the bands nor identify the likely myriad of interacting levels in the spectrum.

IV. FURTHER DISCUSSION

In the above, we have looked at the assignment of a selection of bands across the lowest ~1350 cm^{-1} of the S_1 state of *m*FT. Clearly, IVR cannot occur for the origin and the very lowest levels, but as discussed in Ref. 10, even below 350 cm^{-1}, there are interactions occurring between vibrations, torsions, and vibtor levels. Here, we have extended the examination of levels, where we see limited interactions are present for levels below 950 cm^{-1}, but significant IVR occurs above this, moving toward the statistical (dissipative) IVR regime; the latter is demonstrated by the presence of a largely unstructured underlying background in both the 2D-LIF and ZEKE spectra recorded at ~960 cm^{-1} and ~1260 cm^{-1}. On top of this underlying background, there are numerous well-resolved bands, showing that in the present experiments, some energy remains localized to particular vibrations, while some is dissipated through a range of motions.

We noted above that Timbers *et al.*[7] have compared the behavior of *m*FT and *p*FT, concluding that at about 1200 cm^{-1}, the

rate of IVR was an order of magnitude faster for *m*FT than for *p*FT, based upon quenching experiments. We have studied *p*FT in a range of internal energies, and we have found that below 1000 cm^{-1}, limited IVR occurs involving both anharmonic and vibration–torsional coupling.[16–18,20,21] At ~1015 cm^{-1}, we found that coupling occurred involving two largely separate overtone levels, providing two routes for energy delocalization in *p*FT,[23] while in the region 1190 cm^{-1}–1240 cm^{-1}, there was more widespread IVR, but two levels less than 40 cm^{-1} apart behaved significantly differently.[17,22] In both of the latter, there were still structured bands on top of a broad background, suggesting at least some energy remains localized. In the case of *p*Xyl, however, at these energies, most structure was lost in the ZEKE spectra recorded, suggesting almost complete delocalization of energy; these observations were discussed in terms of symmetry and the density of states (DOS).[17] It was concluded that although the DOS buildup is critical in providing pathways to widespread IVR, this is determined largely by the presence of one or more methyl groups, rather than the symmetry per se. On top of this, the DOS buildup is not smooth, and so at lower internal energies, serendipity can play a large role in determining whether a particular vibration is located in a "clump" of levels; even then, there needs to be a means of efficient coupling to these. Such coupling will clearly depend on symmetry, but also on the motions involved; such considerations lead to the "Tier Model" of IVR, whereby coupling between particular levels is efficient and facilitates pathways to coupling with a wide range of "bath states."[1]

Here, we make further comparison between *m*FT and *p*FT. In Fig. 11, we show their DOS plots for totally symmetric vibrations, and also when including torsions and vibtor levels. It is clear that for *m*FT, there are more totally symmetric vibrations, as all in-plane vibrations are totally symmetric, while for *p*FT, these split into a_1' (a_1 in C_{2v}) and a_1'' (b_2 in C_{2v}) subgroups— this is evident in Fig. 11.

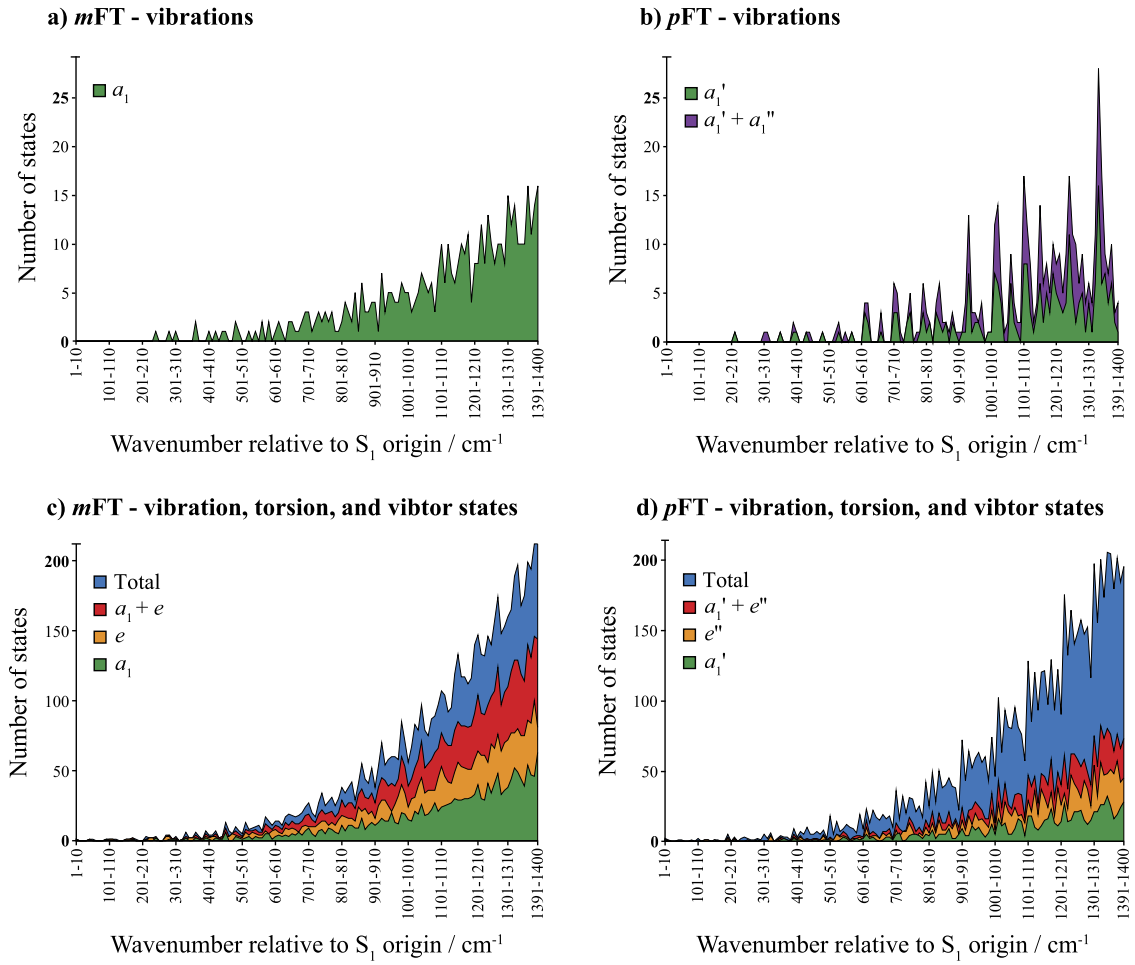

FIG. 11. Density of states (DOS) plots for *m*FT and *p*FT, using calculated vibrational wavenumbers from Table III and Ref. 23. In plots (a) and (b), only vibrational levels are included, while in plots (c) and (d), vibrations and vibtor and torsional levels are included. In both plots, we indicate levels that are accessible from the $m = 0$ and $m = 1$ levels, which are those that are the most populated in the free-jet expansion ($a_1 + e$ for *m*FT and $a_1' + e''$ for *p*FT), together with all levels. Note that we do not consider rotational levels in this work.

Notably, the buildup in the DOS is more erratic for *p*FT than for *m*FT. This difference is clearer once vibtor levels are included, where again an approximate doubling of the available energy levels is seen for *m*FT compared to *p*FT, for levels accessible from $m = 0$ and $m = 1$. Furthermore, it can be seen that the buildup of levels is generally more continuous once vibtor levels are included compared to only the vibrations, which is somewhat erratic, particularly for the totally symmetric levels in *p*FT.

With regard to previous IVR experiments on *p*FT, there has been some uncertainty regarding the vibrations excited, which has been discussed.[45] For *p*FT, there are two main fundamentals at 1196 cm^{-1} and 1232 cm^{-1}, but there are other levels nearby, as examined in depth in our recent work.[22] In Ref. 7, it seems the latter level is excited, which is the 5^1 vibration, mainly corresponding to an in-phase stretch of the C–F and C–CH_3 bonds, with the former motion dominating.[25] As we have discussed in the present work, for *m*FT, the 1260 cm^{-1} transition is assigned as the vibronically induced 11^1, which is largely a ring-based distortion. As such, the vibrational motion is quite different for the two molecules, making the comparison less straightforward. Indeed, the motion of D_{11} (see Fig. 10) in *m*FT will involve the adjacent C–H bonds interacting with the methyl group more strongly than for the 5^1 vibration in *p*FT, which would be one explanation for the increased IVR as a result of vibration–torsional coupling.

In the experiments by Parmenter's group,[7] reliance is placed upon collisional quenching with O_2. The idea is that the excited electronic state is vibrationally excited following laser excitation and that there is time dependence for the IVR to occur. In addition, the higher the partial pressure of O_2, the more rapid the quenching, and the less the time molecule had to undergo IVR. However, this can only occur with levels that are excited coherently within the width of the laser pulse, which will be a few cm^{-1} for a nanosecond pulse (not stated in Ref. 7, but the laser system mentioned suggests this was the case). In Ref. 7, a fit is made to the data to determine k_{IVR}, with electronic and vibrational collision quenching, k_V, included. Various assumptions were made in determining k_{IVR}, with the end conclusion being that this was roughly an order of magnitude larger than that for *p*FT. A discussion of the possible rationalization of this observation was then made, including the DOS of the coupled vibrational levels, the effect of the methyl rotor not being on a principal axis, and the magnitude of the torsional barrier.

With regard to the DOS, we note that there are two factors that increase this in *m*FT relative to *p*FT, both related to the reduction in molecular (point group) symmetry from G_{12} (C_{2v}) for *p*FT to G_6 (C_s) for *m*FT. For the vibrations, using molecular symmetry group labels, *m*FT will have a greater number of totally symmetric vibrations as both the a_1' and a_1'' symmetry vibrations in *p*FT have the same symmetry (a_1) in *m*FT; Fig. 11 indicates that the number of a_1 vibrations in *m*FT is comparable to the number of $a_1' + a_1''$ symmetry vibrations in *p*FT but with a smoother buildup for *m*FT. Furthermore, considering molecular symmetry, the number of *e* torsional levels in *m*FT is about the same as the number of $e' + e''$ torsional levels in *p*FT. Taken together, see Fig. 11, it can be seen that the *total* number of vibrational + vibtor levels is about the same in *p*FT and *m*FT. However, considering only the states that have the same symmetries as the $m = 0$ and $m = 1$ levels (the ones with the dominant populations in the free-jet expansion), then there are about twice as many levels for *m*FT as for *p*FT.

The aforementioned DOS does not include rotational levels, and it was argued in Ref. 7 that coupling with rotational levels would be more significant in *m*FT than *p*FT; if so, then it may be that there is an effect from the use of room temperature and high pressure conditions in Ref. 7, where rotational effects would be expected to be more significant than they would be in jet-cooled, gas-phase studies.[45] It was also commented in that work[7] that at the internal energies employed, *p*FT will couple to 10–50 levels, while *m*FT will couple to essentially an infinite number. The DOS plots in Fig. 11 do not support this latter comment and, further, the 2D-LIF spectra do not either, where the structure is seen, albeit on a background, for both *p*FT (Ref. 19) and *m*FT (present work); this is in contrast to the fluorescence spectrum for *m*FT reported in Ref. 7, where no structure is evident when the quencher is absent.

We concur with the comments in Ref. 7 that the significantly higher barrier in *m*FT is expected to produce larger torsion–vibration coupling terms. One rationale for the higher barrier in *m*FT compared to *p*FT is in terms of hyperconjugation: in *p*FT, hyperconjugation is not expected to be a large effect and weaker van der Waals type interactions are thus expected to dominate, explaining the lower torsional barrier.

As noted above, there has been some ambiguity in the levels employed for IVR studies on *p*FT,[45] which is pertinent as the vibrational motion is expected to be critical in the observed coupling. For *p*FT, at 1200 cm^{-1}, a rather different time-dependent behavior has been observed for the two main levels,[46,47] which was discussed in terms of a rotation-dependent vibration–torsion interaction that occurred specifically for one of the *m* levels. Rotational dephasing was concluded to be a time-dependent effect only and is not seen in frequency-resolved experiments.[19]

In summary, direct comparison between different isomers of substituted benzene molecules is difficult because of the different forms of the vibrations, even if the observed activity seems quite similar. Furthermore, the conditions used in an experiment are expected have a strong bearing on the results,[45] and so caution is strongly advised when making general deductions from a single experiment. Having the ability to resolve vibrational, vibtor, and torsional structures in a spectrum does seem to give the ability to identify explicit coupling channels, but only when the coupling is reasonably limited. Once the coupling becomes widespread, however, this advantage is lost in frequency-resolved experiments if the resolution is not sufficient to resolve all features, or if the spectrum becomes too complicated to assign definitively. Time-resolved photoelectron spectroscopy experiments with picosecond pulses can, however, still be useful in picking out zero-order state contributions in such circumstances, as long as the frequency resolution can be maintained at tens of cm^{-1}.[46,47]

V. CONCLUSIONS

We have presented 2D-LIF and ZEKE spectra obtained when exciting through selected levels up to 1350 cm^{-1} in the lower wavenumber region of the $S_1 \leftarrow S_0$ excitation in *m*FT. We have assigned the majority of the main features observed, but there are many weak features and also broad unstructured backgrounds in some cases. The assigned features confirm that there is widespread vibtor coupling occurring in this molecule, as well as some anharmonic vibrational coupling; these become more prevalent to

higher internal energies and are more common for the *e* symmetry torsional levels than for the a_1 symmetry levels. Explicit couplings can be identified in some cases, while, in others, only potential couplings have been suggested, based upon some of the observed 2D-LIF bands. When there are numerous couplings, the ZEKE spectra become very difficult to assign, owing to the number of bands arising, also causing each to have a lower intensity, and these are located on a rising unstructured background.

Comparing *p*FT and *m*FT, we agree with many, but not all, of the ideas expressed in Ref. 7, but we have highlighted that both the number of vibrations and also torsions, and so vibtor, levels are responsible for the stark increase in the DOS; of course, all of these levels will have an associated set of rotational levels, and hence in room temperature studies, this difference will be exacerbated compared to experiments employing a free-jet expansion. We have emphasized that it is difficult to compare these molecules directly, with the particular vibration excited at ~1250 cm^{-1} being different for the two molecules. Moreover, relying on Wilson/Varsányi labels to identify a vibration can be misleading, since the motions of the atoms for a particular vibrational wavenumber can be very different for *meta* and *para* substituted molecules as discussed in Ref. 27. Last, the buildup in vibrational levels is somewhat erratic at these low wavenumbers, and this suggests that at low energies, notwithstanding the more-rapid buildup in the DOS for *m*FT, the rapidity with which IVR efficiency can increase is restricted since coupling elements will still depend on Δv being small.

Our conclusion is that it seems clear that *m*FT undergoes more rapid IVR than *p*FT, but ascertaining the precise reasons for this, and quantifying them, is far from straightforward.

ACKNOWLEDGMENTS

We are grateful to the EPSRC for funding (Grant No. EP/L021366/1). The EPSRC and the University of Nottingham are thanked for studentships to D.J.K. and A.R.D. Alan Rees, Lewis G. Warner, and Elizabeth F. Fryer are thanked for helping with the recording of some of the spectra during undergraduate projects, with L.G.W. also being grateful for an Undergraduate Summer Bursary funded via a University of Nottingham School of Chemistry 1960 scholarship. The REMPI spectrum of *m*DFB was recorded in our laboratory by Adrian M. Gardner and William D. Tuttle. We are grateful for access to the High-performance computing resource at the University of Nottingham.

DATA AVAILABILITY

The data that support the findings of this study are available from the corresponding author upon reasonable request.

REFERENCES

[1] D. J. Nesbitt and R. W. Field, J. Phys. Chem. **100**, 12735 (1996).
[2] G. M. Roberts and V. G. Stavros, in *Ultrafast Phenomena in Molecular Sciences*, edited by R. de Balda and L. Bañares (Springer, Dordrecht, 2014).
[3] Y. He, C. Wu, and W. Kong, J. Phys. Chem. A **107**, 5145 (2003).
[4] C. S. Byskov, F. Jensen, T. J. D. Jørgensen, and S. B. Nielsen, Phys. Chem. Chem. Phys. **16**, 15831 (2014).
[5] F. Duschinsky, Acta Phys. - Chim. U.R.S.S. **7**, 551 (1937).
[6] L. Martinez-Fernandez, A. Banyasz, L. Esposito, D. Markovitsi, and R. Improta, Signal Transduct. Target Ther. **2**, 17201 (2017).
[7] P. J. Timbers, C. S. Parmenter, and D. B. Moss, J. Chem. Phys. **100**, 1028 (1994).
[8] D. J. Kemp, E. F. Fryer, A. R. Davies, and T. G. Wright, J. Chem. Phys. **151**, 084311 (2019).
[9] D. J. Kemp, L. G. Warner, and T. G. Wright, J. Chem. Phys. **152**, 064303 (2020).
[10] L. D. Stewart, J. R. Gascooke, and W. D. Lawrance, J. Chem. Phys. **150**, 174303 (2019).
[11] K. Okuyama, N. Mikami, and M. Ito, J. Phys. Chem. **89**, 5617 (1985).
[12] K. Takazawa, M. Fujii, T. Ebata, and M. Ito, Chem. Phys. Lett. **189**, 592 (1992).
[13] M. Ito, K. Takazawa, and M. Fujii, J. Mol. Struct. **292**, 9 (1993).
[14] K. Takazawa, M. Fujii, and M. Ito, J. Chem. Phys. **99**, 3205 (1993).
[15] A. R. Davies, D. J. Kemp, L. G. Warner, E. F. Fryer, A. Rees, and T. G. Wright, J. Chem. Phys. **152**, 214303 (2020).
[16] A. M. Gardner, W. D. Tuttle, L. Whalley, A. Claydon, J. H. Carter, and T. G. Wright, J. Chem. Phys. **145**, 124307 (2016).
[17] W. D. Tuttle, A. M. Gardner, L. E. Whalley, D. J. Kemp, and T. G. Wright, Phys. Chem. Chem. Phys. **21**, 14133 (2019).
[18] A. M. Gardner, W. D. Tuttle, L. E. Whalley, and T. G. Wright, Chem. Sci. **9**, 2270 (2018).
[19] D. J. Kemp, W. D. Tuttle, A. M. Gardner, L. E. Whalley, and T. G. Wright, J. Chem. Phys. **151**, 064308 (2019).
[20] W. D. Tuttle, A. M. Gardner, L. E. Whalley, and T. G. Wright, J. Chem. Phys. **146**, 244310 (2017).
[21] D. J. Kemp, A. M. Gardner, W. D. Tuttle, and T. G. Wright, Mol. Phys. **117**, 3011–3026 (2019).
[22] D. J. Kemp, L. E. Whalley, A. M. Gardner, W. D. Tuttle, L. G. Warner, and T. G. Wright, J. Chem. Phys. **150**, 064306 (2019).
[23] A. M. Gardner, L. E. Whalley, D. J. Kemp, W. D. Tuttle, and T. G. Wright, J. Chem. Phys. **151**, 154302 (2019).
[24] A. M. Gardner and T. G. Wright, J. Chem. Phys. **135**, 114305 (2011).
[25] A. Andrejeva, A. M. Gardner, W. D. Tuttle, and T. G. Wright, J. Mol. Spectrosc. **321**, 28 (2016).
[26] W. D. Tuttle, A. M. Gardner, A. Andrejeva, D. J. Kemp, J. C. A. Wakefield, and T. G. Wright, J. Mol. Spectrosc. **344**, 46 (2018).
[27] D. J. Kemp, W. D. Tuttle, F. M. S. Jones, A. M. Gardner, A. Andrejeva, J. C. A. Wakefield, and T. G. Wright, J. Mol. Spectrosc. **346**, 46 (2018).
[28] E. B. Wilson, Jr., Phys. Rev. **45**, 706 (1934).
[29] G. Varsányi, *Assignments of the Vibrational Spectra of Seven Hundred Benzene Derivatives* (Wiley, New York, 1974).
[30] R. S. Mulliken, J. Chem. Phys. **23**, 1997 (1955).
[31] G. Herzberg, *Molecular Spectra and Molecular Structure. II. Infrared and Raman Spectra of Polyatomic Molecules* (Krieger, Malabar, 1991).
[32] W. D. Tuttle, A. M. Gardner, and T. G. Wright, Chem. Phys. Lett. **684**, 339 (2017).
[33] P. A. Graham and S. H. Kable, J. Chem. Phys. **103**, 6426 (1995).
[34] V. L. Ayles, C. J. Hammond, D. E. Bergeron, O. J. Richards, and T. G. Wright, J. Chem. Phys. **126**, 244304 (2007).
[35] N. J. Reilly, T. W. Schmidt, and S. H. Kable, J. Phys. Chem. A **110**, 12355 (2006).
[36] J. R. Gascooke and W. D. Lawrance, Eur. Phys. J. D **71**, 287 (2017).
[37] J. H. S. Green, Spectrochim. Acta. **26A**, 1523 (1970).
[38] A. M. Gardner, W. D. Tuttle, P. Groner, and T. G. Wright, J. Chem. Phys. **146**, 124308 (2017).
[39] M. J. Frisch, G. W. Trucks, H. B. Schlegel, G. E. Scuseria, M. A. Robb, J. R. Cheeseman, G. Scalmani, V. Barone, G. A. Petersson, H. Nakatsuji, X. Li, M. Caricato, A. V. Marenich, J. Bloino, B. G. Janesko, R. Gomperts, B. Mennucci, H. P. Hratchian, J. V. Ortiz, A. F. Izmaylov, J. L. Sonnenberg, D. Williams-Young, F. Ding, F. Lipparini, F. Egidi, J. Goings, B. Peng, A. Petrone, T. Henderson, D. Ranasinghe, V. G. Zakrzewski, J. Gao, N. Rega, G. Zheng, W. Liang, M. Hada, M. Ehara, K. Toyota, R. Fukuda, J. Hasegawa, M. Ishida, T. Nakajima, Y. Honda, O. Kitao, H. Nakai, T. Vreven, K. Throssell, J. A. Montgomery, Jr., J. E. Peralta, F. Ogliaro, M. J. Bearpark, J. J. Heyd, E. N. Brothers, K. N. Kudin, V. N. Staroverov, T. A. Keith, R. Kobayashi, J. Normand, K. Raghavachari, A. P. Rendell, J. C. Burant, S. S. Iyengar, J. Tomasi, M. Cossi, J. M. Millam, M. Klene, C. Adamo, R. Cammi, J. W. Ochterski, R. L. Martin, K. Morokuma, O. Farkas, J. B. Foresman, and D. J. Fox, Gaussian 16, Revision A.03, Gaussian, Inc., Wallingford CT, 2016.

[40]E. Fermi, Z. Phys. **71**, 250 (1931).
[41]N. T. Whetton and W. D. Lawrance, J. Phys. Chem. **93**, 5377 (1989).
[42]J. R. Gascooke and W. D. Lawrance, J. Chem. Phys. **138**, 134302 (2013).
[43]A. R. Davies, D. J. Kemp, and T. G. Wright (unpublished).
[44]D. J. Kemp, A. M. Gardner, W. D. Tuttle, J. Midgley, K. L. Reid, and T. G. Wright, J. Chem. Phys. **149**, 094301 (2018).
[45]C. J. Hammond, V. L. Ayles, D. E. Bergeron, K. L. Reid, and T. G. Wright, J. Chem. Phys. **125**, 124308 (2006).
[46]J. A. Davies, A. M. Green, A. M. Gardner, C. D. Withers, T. G. Wright, and K. L. Reid, Phys. Chem. Chem. Phys. **16**, 430 (2014).
[47]J. A. Davies, L. E. Whalley, and K. L. Reid, Phys. Chem. Chem. Phys. **19**, 5051 (2017).